

Interface-induced phenomena in polarization response of ferroelectric thin films

A. K. Tagantsev and G. Gerra

Citation: *J. Appl. Phys.* **100**, 051607 (2006); doi: 10.1063/1.2337009

View online: <http://dx.doi.org/10.1063/1.2337009>

View Table of Contents: <http://jap.aip.org/resource/1/JAPIAU/v100/i5>

Published by the [American Institute of Physics](#).

Additional information on J. Appl. Phys.

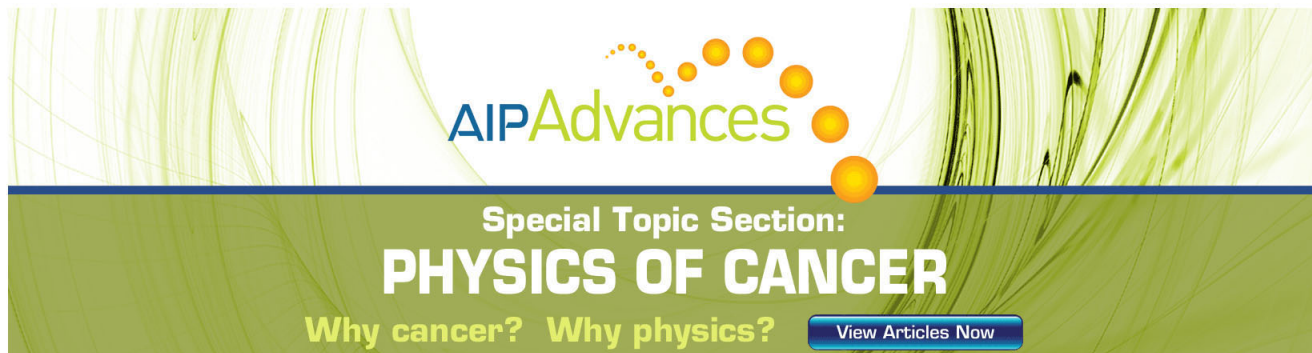
Journal Homepage: <http://jap.aip.org/>

Journal Information: http://jap.aip.org/about/about_the_journal

Top downloads: http://jap.aip.org/features/most_downloaded

Information for Authors: <http://jap.aip.org/authors>

ADVERTISEMENT

The advertisement features a green and yellow color scheme. At the top, the text 'AIPAdvances' is displayed in a stylized font, with a series of yellow dots forming an arc above the word 'Advances'. Below this, the text 'Special Topic Section: PHYSICS OF CANCER' is written in a bold, white, sans-serif font. At the bottom, the phrase 'Why cancer? Why physics?' is written in a yellow, sans-serif font, followed by a blue button with the text 'View Articles Now' in white. The background of the advertisement is a green and yellow abstract pattern.

AIPAdvances

Special Topic Section:
PHYSICS OF CANCER

Why cancer? Why physics? [View Articles Now](#)

Interface-induced phenomena in polarization response of ferroelectric thin films

A. K. Tagantsev^{a)} and G. Gerra*Ceramics Laboratory, Swiss Federal Institute of Technology (EPFL), CH-1015 Lausanne, Switzerland*

(Received 21 March 2006; accepted 28 June 2006; published online 12 September 2006)

This article reviews the existing theoretical models describing the interface-induced phenomena which affect the switching characteristics and dielectric properties of ferroelectric thin films. Three groups of interface-induced effects are addressed—namely, “passive-layer-type” effects, ferroelectric-electrode contact potential effects, and the poling effect of the ferroelectric-electrode interface. The existing experimental data on dielectric and switching characteristics of ferroelectric thin film capacitors are discussed in the context of the reviewed theories. Special attention is paid to the case of internal bias field effects. © 2006 American Institute of Physics.

[DOI: [10.1063/1.2337009](https://doi.org/10.1063/1.2337009)]

I. INTRODUCTION

Technological applications are pushing the size of practical devices down to nanorange. At such scales, neglecting size effects becomes clearly unacceptable. While well-developed theories exist for bulk materials, their extensions to thin films and small particles are often less advanced. Ferroelectricity is one class of physical systems where the difference in behavior exhibited by thin films as opposed to bulk materials is still not fully understood. Though it is clear that the origin of such difference lies in the enhanced importance of size effects at small thicknesses, we are far from grasping the whole picture, and most of all we are far from being able to predict the switching properties and piezoelectric response of thin film systems with given deposition conditions and composition. One step towards the understanding of the subject involves a rigorous analysis of all the possible scenarios leading to finite size effects.

In ferroelectric materials for electronic applications, size effects are due primarily to the interface between the electrode and the ferroelectric. The presence of the interface is clearly felt in piezoelectric and dielectric measurements as a passive layer reducing the permittivity of the system, as an offset of the polarization and/or voltage, as a bias field causing an asymmetry in the switching properties, and as a location of favorable nucleation seeds. In this paper, we present a review of all the possible known mechanisms describing the influence of the ferroelectric-electrode (or ferroelectric-substrate) interface on the polarization response of the material.

In Sec. II A, we develop the idea that a thin layer of nonswitchable insulating material—the “passive layer”—may exist in the nearby-electrode regions, giving rise to certain characteristics in the measured hysteresis loops of thin films. In Sec. II B, we consider the case of finite conduction in the passive layer, and related effects on hysteresis. In Secs. II C and II D, we discuss the intrinsic and the domain contribution to permittivity due to the presence of the passive

layer, while in Sec. II E we analyze the relationship between a passive layer and imprint. Section III is devoted to the phenomenon of depletion, which is due to the electrochemical interaction between a metal (the electrode) and a semiconductor (the ferroelectric). Its effects on switching and on permittivity are reviewed. In Sec. IV, we consider the possible implications of poling (i.e., fixing or enhancement of polarization) at the interface on the switching, on the nucleation of reverse domains, and on the dielectric permittivity. Section V is dedicated to a discussion of experimental evidence for the internal bias field effects in ferroelectric thin films in the context of available theoretical models.

II. PASSIVE LAYER MODELS

A. Hysteresis and insulation passive layer

It is a known fact that the permittivity of a ferroelectric decreases with decreasing thickness. This observation can be explained by assuming the existence of a thin layer of non-switchable dielectric material (whose dielectric constant is much less than that of the ferroelectric) connected in series with the ferroelectric.^{1–3} We call this layer of nonferroelectric dielectric material a passive layer. Let us consider the sandwich structure shown in Fig. 1. Neglecting the possible inhomogeneity of the electric field in the plane of the capacitor, its switching behavior can be analyzed starting from the condition of continuity of the normal component of the electric displacement field and from the equation for the potential drop across the system:

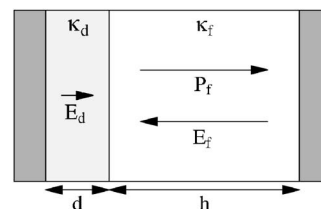


FIG. 1. Electrode-passive layer-ferroelectric-electrode sandwich structure. The thickness of the passive layer is d , that of the ferroelectric is h .

^{a)}Electronic mail: alexander.tagantsev@epfl.ch

$$\varepsilon_0 \kappa_d E_d = \varepsilon_0 E_f + P_f, \quad (2.1)$$

$$dE_d + hE_f = (d + h)E,$$

where E is the applied field; P_f and E_f are the average polarization and electric field in the ferroelectric, h being its thickness; E_d , d , and κ_d are the average field in the dielectric, its thickness, and dielectric constant, respectively. For the case of a thin passive layer ($d \ll h$) we are interested in, Eq. (2.1) can be reduced to a set of simple equations relating the polarization and the field in the ferroelectric to the field applied to the sandwich and to the average polarization in it, P (the quantity that is actually measured). Neglecting the difference between the polarization and the displacement field of the ferroelectric, these equations read

$$E_f = E - \frac{d}{h} E_d, \quad (2.2)$$

$$E_d = \frac{P_f}{\varepsilon_0 \kappa_d},$$

$$P = P_f.$$

Equations (2.2) enable calculations of a set of hysteresis loops $P(E, E_m)$ for the sandwich at different amplitudes E_m of the driving field E , if the set $P_f(E_f, E_{fm})$ is known for the ferroelectric. The scheme of the calculations is as follows. To obtain the loops of the sandwich for a given value of E_m (say, E_1) one first determines the amplitude E_{fm} of the driving field seen by the ferroelectric when the amplitude E_m of the applied driving field equals E_1 . This value of E_{fm} , which we will call E_2 , can be found as a root of the equation

$$E_{fm} = E_1 - \frac{d}{\varepsilon_0 \kappa_d h} P_f(E_{fm}, E_{fm}). \quad (2.3)$$

The polarization and the field in the ferroelectric during the considered cycling are thus related by the function $P_f = P_f(E_f, E_2)$, so that the loops exhibited by the sandwich can be generated using the equations

$$E_f = E - \frac{d}{\varepsilon_0 \kappa_d h} P_f(E_f, E_2), \quad (2.4)$$

$$P = P_f(E_f). \quad (2.5)$$

This approach was applied for modeling hysteresis loops of a sandwich containing ferroelectric films whose set of hysteresis loops was available from experiment. The results of such modeling¹ are presented in Fig. 2(a). (The gap seen on the calculated loops is an artifact of the calculations, which use an experimental set of loops measured with a single voltage cycle, where a gap in the loop at remanence often occurs.) Comparing the loop for the ferroelectric with those for the sandwich with different thicknesses of the passive layer, the following trends can be recognized. An increase of the passive layer thickness (or a decrease of the thickness of the ferroelectric) results in (i) an essential tilt of the loops, (ii) an essential reduction of the remanent polarization P_r , (iii) a certain reduction of the maximal polarization on the loop P_m ,

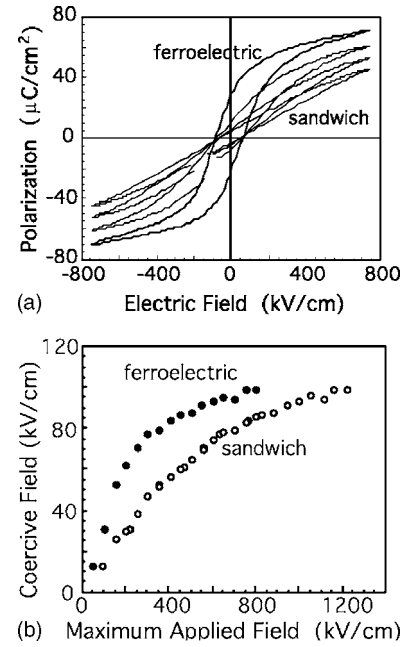


FIG. 2. (a) Hysteresis loop of a ferroelectric, and the calculated loops of the sandwich for different values of $d/\kappa_d h = 0.003, 0.009, 0.018$. (b) The calculated field amplitude dependence of the coercive field for the sandwich structure (ferroelectric-thin passive layer) with $d/\kappa_d h = 0.01$, compared to that of the ferroelectric part.

and (iv) a certain reduction of the coercive field E_c . Analytical treatment of the problem¹ confirmed such remarks. It was also shown that, in the limit of high amplitudes of the driving field E_m (for which the polarization loops seen by the ferroelectric become fully saturated), effects (iii) and (iv) disappear whereas effects (i) and (ii) still hold. For the coercive field, this trend is illustrated in Fig. 2(b). While referring the reader to the original paper¹ for details of the analysis, we would like to comment here only two issues: the tilt of the loop and the behavior of E_c .

To characterize the tilt of the loop it is convenient to consider, as a measure of the tilt, its slope at E_c —i.e., the effective dielectric permittivity of the sandwich structure measured at this point, $\kappa_s(P=0)$. Using Eqs. (2.2), this parameter can be related to the corresponding parameter from the loop of the ferroelectric, $\kappa_f(P_f=0)$:

$$\frac{h}{\kappa_s(P=0)} = \frac{h}{\kappa_f(P_f=0)} + \frac{d}{\kappa_d}, \quad (2.6)$$

where one can easily recognize the formula for in-series connection of two capacitors (in the case $h \gg d$) applied to the considered structure.^{4,5} Equation (2.6) clearly explains the aforementioned relation between d (or h) and the tilt of the polarization loop of the sandwich [cf. Fig. 3, where the inverse tilt at coercivity, $\kappa_s(P=0)^{-1}$, is plotted against the inverse thickness, h^{-1} , for a set of PZT films].

The impact of the passive layer on the coercive field of the system, which is illustrated in Fig. 2(b), is less evident than in the case of the loop tilt. Actually, this result seems contradictory to routine reasoning: The coercive field is roughly the field needed to switch the ferroelectric. There is a drop of potential across the passive layer. Therefore, a higher voltage should be applied to the sandwich than to the

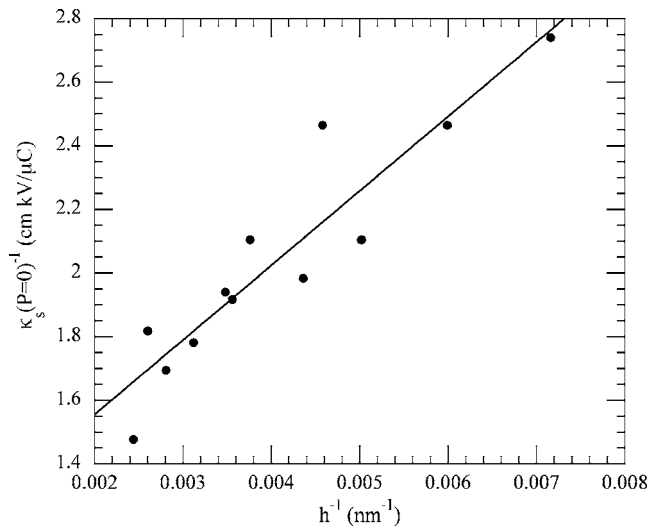


FIG. 3. Inverse tilt of the polarization loop at E_c , $\kappa_s(P=0)^{-1}$, vs inverse thickness of the film, h^{-1} , for a set of 53/47 PZT sol-gel films. The data seem to validate the passive layer model prediction of a linear dependence of the two quantities—cf. Eq. (2.6). After Ref. 5.

bare ferroelectric in order to switch it. For this reason, one might expect the coercive field to increase with increasing thickness of the passive layer.^{6–8} We elucidate the origin of the effect shown in Fig. 2(b) by pointing out a drawback of the above reasoning. First, according to Eq. (2.2), the drop of potential across the passive layer equals $Pd/\epsilon_0\kappa_d$, so that at E_c (where $P=0$) it vanishes—within the accuracy of the calculations. Thus, the field seen by the ferroelectric and that seen by the sandwich at E_c is the same. It follows that if the loop exhibited by the ferroelectric part of the sandwich is saturated (i.e., if P_r and E_c of the loop are virtually independent of driving field amplitude), then the coercive fields of the ferroelectric and of the sandwich are equal [cf. Fig. 2(b)]. The case where the loop exhibited by the ferroelectric part of the sandwich is not saturated requires a more involved treatment which shows that, in this regime, E_c is a decreasing function of $d/\kappa_d h$. This behavior is related to the fact that the loop exhibited by the ferroelectric part of the sandwich is driven by a field whose amplitude is smaller than that of the field applied to the whole sandwich structure, and for smaller driving field amplitudes [the abscissa in Fig. 2(b)] the coercive field [the y coordinate in Fig. 2(b)] is smaller.

B. Hysteresis and insulation passive layer with threshold conduction

An estimate of the electric field acting on the passive layer E_d during switching (for a capacitor containing a thin film of a conventional ferroelectric such as PZT) shows that it can be very large. For example, taking $P=0.3 \text{ C/m}^2$ and the dielectric permittivity of the passive layer as high as $\kappa_d=100$, one finds $E_d=3 \text{ MV/cm}$. This field is large enough to induce considerable charge injection across the layer. Thus, an adequate description of the switching in a ferroelectric capacitor may require taking into account this injection, as well as the influence of the injected charge on the injection itself.^{9,10} This phenomenon can be readily incorporated into the model considered above by taking into account (i) the

free carrier transport across the layer, $J(E_d)$ being the current density across the layer, and (ii) the accumulation of these free carriers at the ferroelectric-dielectric interface, σ being the corresponding surface charge density. An essential feature brought about by the introduction of the injection into the model is an effective screening of the polarization of the ferroelectric by the charge of the accumulated carriers.

The switching behavior of the system is then described by a modified version of Eqs. (2.2), appended with the equation for the charge transport across the thin ($d \ll h$) layer:

$$E_f = E - \frac{d}{h} E_d, \quad (2.7)$$

$$E_d = \frac{P_f - \sigma}{\epsilon_0 \kappa_d}, \quad (2.8)$$

$$P = P_f, \quad (2.9)$$

$$\frac{d\sigma}{dt} = J(E_d). \quad (2.10)$$

Here, the screening effect of the charge at the ferroelectric-dielectric interface is clearly seen in Eq. (2.8). This screening results in a reduction of the field in the passive layer. According to Eq. (2.9), the total polarization of the sandwich is taken to be equal to the polarization of the ferroelectric layer P —i.e., the contribution of the dielectric layer is neglected.¹¹ The complete description of the problem is given by Eqs. (2.7) and (2.10) along with the explicit dependences of $J(E_d)$ and $P_f(E_f)$.

Following Ref. 10, we will discuss the impact of this kind of passive layer on the coercive field of the sandwich. For simplicity, we consider the case of saturated loops, for which, in the previous model, E_c of the sandwich was found to be independent of layer thickness and equal to the coercive field of the ferroelectric E_{c0} . As for the $J(E_d)$ dependence, we assume it to be very steep and characterized by a threshold field E_{th} . In other words, in this model, if in the surface dielectric layer $E_d < E_{th}$, the layer behaves as an insulator, whereas if $E_d > E_{th}$ the layer behaves as a nonlinear conductor, maintaining E_d very close to E_{th} (slightly higher), irrespective of the passing current. This is a reasonable approximation for typical injection mechanisms in thin dielectric films.

The impact of this kind of passive layer on E_c can be readily elucidated from the following consideration. The behavior of the system differs depending on the relation between E_{th} and the maximal polarization P_m on the hysteresis loop. If $E_{th} > P_m/\epsilon_0\kappa_d$, the field in the surface layer $E_d = P_f/\epsilon_0\kappa_d$ [see Eq. (2.8), where $\sigma=0$ before the onset of injection] is always smaller than the injection threshold field, so that the injection is off during the cycling and the surface layer behaves as an ideal insulator. In this case, the model reduces to the insulating layer model treated previously and we find no effect of the passive layer on the coercive field, i.e.,

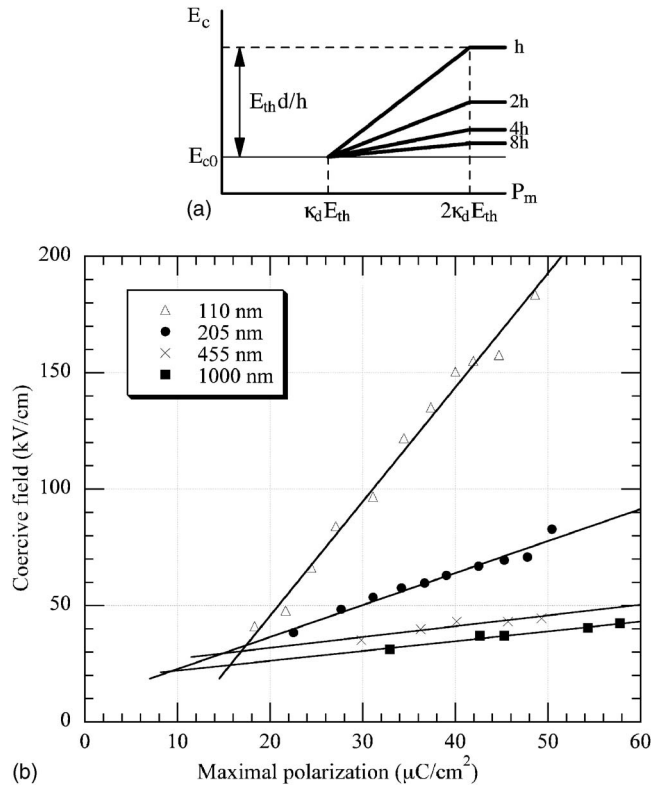


FIG. 4. (a) Predicted dependence of the coercive field E_c on maximum polarization P_m and on film thickness h according to the insulating passive layer with threshold conduction model; and (b) experimental confirmation of the prediction for $\text{Pb}(\text{Zr}_{0.45}\text{Ti}_{0.55})\text{O}_3$ films with Pt electrodes. After Ref. 10.

$$E_c = E_{c0}. \quad (2.11)$$

If $E_{th} < P_m / \epsilon_0 \kappa_d$, the field in the surface layer E_d will reach the threshold value E_{th} during cycling and injection will be on during some phases of the switching cycle. This injection will accumulate charge at the ferroelectric-dielectric interface, which in turn will affect the value of the coercive field of the sandwich, E_c . It has been shown¹⁰ that for $\epsilon_0 \kappa_d E_{th} < P_m < 2\epsilon_0 \kappa_d E_{th}$,

$$E_c = E_{c0} + \frac{d}{\epsilon_0 \kappa_d h} (P_m - \epsilon_0 \kappa_d E_{th}), \quad (2.12)$$

and, for $P_m > 2\epsilon_0 \kappa_d E_{th}$,

$$E_c = E_{c0} + \frac{d}{h} E_{th}. \quad (2.13)$$

The physical difference between the regimes corresponding to Eqs. (2.12) and (2.13) is that, in the first case, the injection is on during some phases of the switching cycle but it is off at the coercive field point whereas, in the second case, the injection is also on at this point. It is seen from these equations that the injection implies a thickness dependence of the coercive field of the sandwich and, in the first regime, an additional P_m dependence. These dependences are illustrated in Fig. 4(a).

It is worth noting that a transparent physics is standing behind the trends given by Eqs. (2.12) and (2.13). In the case where the injection is on at E_c —Eq. (2.13)—the field in the passive layer is exactly known and equal to E_{th} , so that this

relation directly follows from a simple calculation of the voltage drop across the sandwich at coercivity: $hE_{c0} + dE_{th}$.⁹ The trend given by relation (2.12)—namely, the increase of E_c with increasing P_m —can be understood from the following argument. At the tip of the loops (i.e., at $P = P_m$), the polarization is screened by a certain amount of charge at the ferroelectric-dielectric interface. When the applied field reduces from its maximum value, this charge holds constant (as we would need a field in the opposite direction and above the threshold value in order to reverse the charge transport) up to the E_c point (since at E_c the injection is still off). At this point ($P = 0$), this charge is no longer compensated by the bound charge due to polarization, and it creates a field that opposes polarization reversal, finally resulting in an increase of E_c . Since the screening charge increases with increasing P_m , E_c increases as well.

A remarkable feature of the theoretical results given by Eq. (2.12) is that its relevance to experimentally observed effects can be verified by analyzing a two-dimensional array of data: E_c as a function of the film thickness h and the maximal polarization P_m . An example of such analysis for a Pt/PZT/Pt thin film capacitor is shown in Fig. 4(b), where it is seen that the experimental results reproduce fairly well the fanlike structure of the graph predicted by the model [Fig. 4(a)].

According to Ref. 10, apart from the description of the size effect in switching in a Pt/PZT/Pt system, the presented model also gives a possible explanation for the much smaller magnitude of this effect in Bi-containing thin films¹² and oxide-electrode systems.⁹ In the first case, a smaller magnitude of the maximal ferroelectric polarization P_m in these materials can be a reason for the absence of nearby-electrode injection and, as a result, for the absence of the size effect on the coercive field [i.e., $P_m < E_{th} \epsilon_0 \kappa_d$ in Fig. 4(a)]. In the case of PZT with oxide electrodes, known for much higher leakage currents than those in the Pt/PZT/Pt system, one could expect a much stronger nearby-electrode injection. In terms of the model, this corresponds to small E_{th} and the regime of relatively large P_m [i.e., $P_m > 2E_{th} \epsilon_0 \kappa_d$ in Fig. 4(a)]. In this regime the magnitude of the size effect is proportional to E_{th} and therefore small. In other words, the injection actually short-circuits the nearby-electrode layer, so that the layer ceases to influence the switching.

C. Passive layer and intrinsic contribution to dielectric permittivity

It is obvious that the dielectric response of a sandwich structure consisting of two (ferroelectric and dielectric) layers is sensitive to the presence of the dielectric layer. In terms of simple electrostatic considerations, it is also clear that the out-of-plane and in-plane components of the effective permittivity of the system are differently affected by this layer, since the first case corresponds to the “in-series” connection of the layers, whereas, in the second case, we can talk about “parallel” connection. Such a consideration leads to well known expressions for the effective permittivity of the system, κ_{eff} :

$$\frac{h+d}{\kappa_{\text{eff}}} = \frac{d}{\kappa_d} + \frac{h}{\kappa} \quad (2.14)$$

and

$$(h+d)\kappa_{\text{eff}} = d\kappa_d + h\kappa \quad (2.15)$$

for the out-of-plane and in-plane cases, respectively. Here, h and d are the thicknesses of the ferroelectric and of the dielectric, and κ and κ_d being their permittivities. These formulas are strictly applicable to the situation where the permittivity of the ferroelectric κ is controlled by the lattice contribution. In the case where the domain contribution to κ is essential, their application may be limited (we will discuss this point in Sec. II D). In situations of practical interest, the dielectric has much smaller thickness and permittivity than the ferroelectric, so that Eqs. (2.14) and (2.15) can be simplified down to the forms

$$\kappa_{\text{eff}}^{-1} = \kappa^{-1} + \frac{d}{h}\kappa_d^{-1}, \quad (2.16)$$

$$\kappa_{\text{eff}} = \kappa \left(\frac{h-d}{h} \right). \quad (2.17)$$

The relations given above may be relevant to the dielectric response of real ferroelectric thin films. Actually, a number of reasons may cause ferroelectric thin films to exhibit a dielectric response identical or similar to that of the sandwich structure discussed above. The simplest possibility is the presence of a secondary phase at the surface of the films. In addition, there exist two intrinsic reasons for this kind of dielectric behavior, which are related to nearby-surface variation of the polarization (field induced or spontaneous) and to the charge distribution in the electrodes. One more source of passive layers is the presence of misfit dislocations.^{13,14}

The charge distribution in the electrodes becomes important when the film is characterized by using a parallel plate capacitor. The origin of the phenomenon is the fact that free charges in the electrode form a layer of finite thickness. For this reason, the center of mass of the charges in the electrode is separated by some distance from the polarization bound charge in the ferroelectric. If the dielectric response of a film is monitored by using a parallel plate capacitor, the free charges in the electrode behave as a capacitor connected in series with the material of the films.^{15,16} Treatment of the electron gas in the electrode in the Thomas-Fermi approximation¹⁷ shows that this capacitor has the capacitance per unit area of ϵ_0/l_s , where l_s is the Thomas-Fermi screening length. This leads to an expression for the apparent out-of-plane dielectric permittivity of the film, which is similar to that given by Eq. (2.16):

$$\kappa_{\text{eff}}^{-1} = \kappa^{-1} + \frac{2l_s}{h}. \quad (2.18)$$

The impact of the nearby-surface variation of the polarization (field induced or spontaneous) on the effective permittivity of the film was first theoretically addressed by Kretschmer and Binder.¹⁸ Below we will present the results

of their theory in the paraelectric phase, which are generalized for the case of nonvanishing background dielectric permittivity of the ferroelectric—which was ignored in their work.

The starting point of the model by Kretschmer and Binder is the assumption that the surface value of the polarization in a ferroelectric is not affected by the applied electric field as strongly as that in the bulk. This is consistent with the microscopic argument that the ferroelectric softness of the lattice is somehow suppressed near the surface. The simplest modeling of this point can be performed in the framework of the continuous Landau theory for a situation where the polarization at the two surfaces of the film is completely blocked. The linear polarization response in this case can be described by using the following equation for the polarization in the film:

$$E = \alpha P - \delta \frac{\partial^2 P}{\partial x^2}, \quad (2.19)$$

with the boundary conditions

$$P(0) = 0 \quad \text{and} \quad P(h) = 0, \quad (2.20)$$

where P is the polarization associated with the soft mode, and the surfaces of the films are at $x=0$ and $x=h$. In the following treatment, we will bear in mind that the relative dielectric permittivity of the material is always large, i.e., $\kappa = (\alpha\epsilon_0)^{-1} \gg 1$.

In the case of the in-plane component of the effective permittivity of the system, which is typically monitored using the planar capacitor setup (with gap g much greater than film thickness h), the expected inhomogeneity of polarization across the film does not create a depolarizing field. Thus, the field E entering Eq. (2.19) is equal to the “applied field” $E_{\text{ext}} = V/g$, where V is the voltage applied to the gap. In this case, the distribution of the polarization across the film can be readily found in the form

$$P(x) = \frac{E_{\text{ext}}}{\alpha} \left\{ 1 - \frac{\cosh[(x-h/2)/\xi]}{\cosh(h/2\xi)} \right\}, \quad (2.21)$$

where

$$\xi = \sqrt{\frac{\delta}{\alpha}} \quad (2.22)$$

is the so-called correlation radius evaluated in the paraelectric phase. Typically, ξ rarely exceeds a few nanometers. For cases of practical interest, where $h \gg \xi$, Eq. (2.21) leads to the following value of the average polarization in the films:

$$\bar{P} = \frac{1}{h} \int_0^h P(x) dx = \frac{E_{\text{ext}}}{\alpha} \left(1 - \frac{2\xi}{h} \right). \quad (2.23)$$

This corresponds to an effective dielectric permittivity of the system

$$\kappa_{\text{eff}} = \kappa \left(\frac{h-2\xi}{h} \right). \quad (2.24)$$

This equation means that, effectively, there are two layers of thickness ξ having the dielectric constant much smaller than κ , so that they do not actually contribute to the polarization

response. Alternatively, these layers can be considered as connected in parallel with a ferroelectric film of thickness $h-2\xi$.

In the case of the out-of-plane component of the effective permittivity of the system, which corresponds to the situation of a parallel plate capacitor, the polarization is normal to the plane of the films and its variation *does create a depolarizing field*. This is a crucial difference compared to the previous case. The relation between the applied field $E_{\text{ext}} = V/h$ and the field seen by the ferroelectric can be found from the Poisson equation. Taking into account the background contribution to the displacement field ($\epsilon_0 \kappa_b E$, where κ_b is the contribution to the electric permittivity from the nonferroelectric lattice modes of the crystal^{19,20} and $\kappa_b \ll \kappa$), the Poisson equation is in our case $d(\epsilon_0 \kappa_b E + P)/dx = 0$, leading to the relation

$$E = E_{\text{ext}} - \frac{1}{\epsilon_0 \kappa_b} (P - \bar{P}). \quad (2.25)$$

Using this relation, Eq. (2.19) can be rewritten as

$$E_{\text{ext}} - \alpha \bar{P} = \left(\alpha + \frac{1}{\epsilon_0 \kappa_b} \right) (P - \bar{P}) - \delta \frac{\partial^2 (P - \bar{P})}{\partial x^2}. \quad (2.26)$$

The solution to this equation satisfying the boundary conditions Eq. (2.20) reads

$$P(x) = \frac{E_{\text{ext}}}{\alpha} \left\{ 1 - \frac{\cosh[(x-h/2)/\xi_1]}{\cosh(h/2\xi_1)} \right\} \times \frac{1}{1 + 2\epsilon(\kappa/\kappa_b)(\xi_1/h)\tanh(h/2\xi_1)}, \quad (2.27)$$

where $\xi_1 = \xi/\sqrt{1+\kappa/\kappa_b} \approx \xi/\sqrt{\kappa/\kappa_b} = \sqrt{\kappa_b} \sqrt{\delta \epsilon_0}$ has the meaning of the scale on which, in this geometry, the polarization changes appreciably near the film surfaces. Note that ξ_1 is smaller than ξ , so that, in any situation of practical interest, $\xi_1/h \ll 1$. Under this conditions, Eq. (2.23) leads to the following expression for the effective dielectric permittivity of the film:

$$\kappa_{\text{eff}}^{-1} = \kappa^{-1} + \kappa_b^{-1} \frac{2\xi_1}{h}. \quad (2.28)$$

This relation corresponds to the in-series connection of the ferroelectric film with two dielectric layers of thickness ξ_1 and dielectric permittivity κ_b .

Thus we see that the surface region with partially suppressed dielectric response behaves as a passive layer; however, in contrast to a real dielectric layer, its thickness is essentially different for in-plane and out-of-plane geometries.

The above theoretical treatment of the problem has been presented for the situation where the polarization at the surfaces of the film is completely blocked—Eq. (2.20). The more general situation, where the blocking is not complete, can be simulated by using the mixed boundary conditions

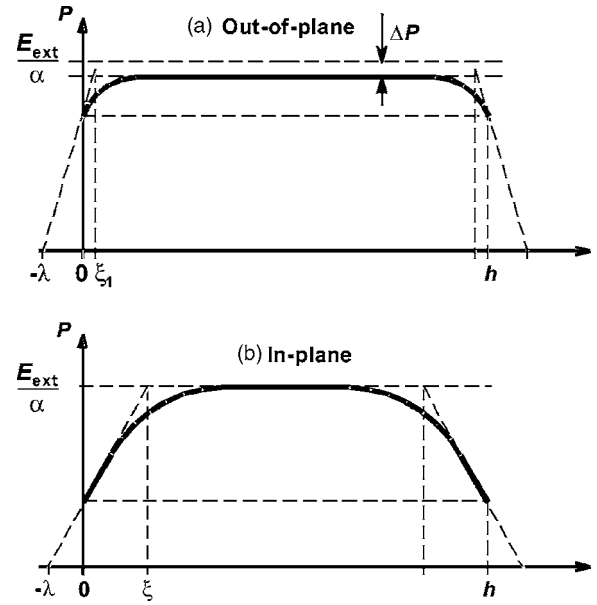


FIG. 5. Schematic distribution of polarization across a film of thickness h for the out-of-plane (a) and in-plane (b) cases. $\Delta P \alpha / E_{\text{ext}} = 2\kappa \xi_1 / \kappa_b h$, where $\xi_1 = \xi \sqrt{\kappa_b / \kappa}$ —cf. Eqs. (2.27) and (2.30). Here, κ is the dielectric constant of the material, κ_b its background dielectric constant, ξ is the correlation length, and E_{ext}/α is the “bulk value” of polarization.

$$P(0) - \lambda \frac{\partial P}{\partial x} \Big|_{x=0} = 0, \quad P(h) + \lambda \frac{\partial P}{\partial x} \Big|_{x=h} = 0. \quad (2.29)$$

These conditions interpolate the situation between blocked (equivalent to $\lambda=0$) and free ($\lambda \rightarrow \infty$) polarizations at the surfaces of the film. After this modification, the above results, Eqs. (2.24) and (2.28), still hold but with the substitutions

$$\xi \Rightarrow \frac{\xi}{1 + \lambda/\xi} \quad \text{and} \quad \xi_1 \Rightarrow \frac{\xi_1}{1 + \lambda/\xi_1}. \quad (2.30)$$

Thus, as one might expect, the weakening of the surface blocking leads to a reduction of the effective passive layer thickness, the effect vanishing in the limit of free polarization at the film surface ($\lambda \rightarrow \infty$).

It is instructive to illustrate schematically the difference between the spatial distributions of the polarization for the “in-plane” and “out-of-plane” situations (Fig. 5). In the in-plane situation, where there is no depolarizing effect, the polarization reaches the “bulk value” E_{ext}/α (i.e., the value expected in a bulk sample for the same value of the applied field E_{ext}) exponentially fast. On the other hand, in the out-of-plane situation, due to depolarizing effects, the polarization changes yet faster with the distance from the electrode, but finally reaches a value which is smaller than the bulk value of polarization. This figure also illustrates the geometrical meaning of parameter λ as the so-called extrapolation length.

All in all, the two models of interfacial polarization blocking predict an increasing thickness dependence of the dielectric permittivity of the films—cf. Eqs. (2.24) and (2.28).

Let us now address the applicability of these predictions to real experimental situations in (Ba,Sr)TiO₃ films, the ma-

material for which the discussed size effect is of practical importance. To do so, some information on the correlation length ξ in the material are needed in addition to its known dielectric parameters. These information may be extracted from the data on dispersion of the soft-mode phonons. Using the data from Refs. 21 and 22, the temperature independent parameter $\xi/\sqrt{\kappa} = \sqrt{\delta\epsilon_0}$ is evaluated²³ as 0.03 Å for BaTiO₃ and 0.08 Å for SrTiO₃. For $\kappa=1600$, this leads to estimates for the correlation radius ξ of 1.2 Å for BaTiO₃ and 3.2 Å for SrTiO₃. These estimates enable us to draw two important conclusions about the applicability of the model.

- (i) For situations of practical interest, the expected thickness dependence of the in-plane component of the measured permittivity is very weak. According to Eq. (2.24), the expected relative correction to the bulk permittivity is about $2\xi/h$. For 200 nm thick films, this makes a 1% correction at most. However, this result may be taken only as a qualitative one since the theoretical situation corresponds to the limit of the range of applicability of the continuous theory; the latter is applicable if the typical scale of the polarization variation (ξ in this case) is substantially larger than the lattice constant of the material [4 Å in the case of (Ba,Sr)TiO₃], which is clearly not the case.
- (ii) For the out-of-plane component of the measured permittivity, a much stronger impact of the surface blocking of the polarization is found. According to Eq. (2.28), the expected relative correction to the bulk permittivity is about $2(\xi_1/h)(\kappa/\kappa_b)$, that is, some $\sqrt{\kappa/\kappa_b}$ times stronger than in the case of the in-plane component. On the other hand, assuming $\kappa_b \approx 10$, the scale $\xi_1 = \sqrt{\kappa_b} \sqrt{\delta\epsilon_0}$ (i.e., 0.1–0.2 Å) is much smaller than the lattice constant of the material, so that the use of this theoretical prediction, even as an order-of-magnitude estimate, cannot be justified. Nevertheless, the physics behind Eq. (2.28)—namely, the in-series connection of the surface passive layer with the “bulk” ferroelectric part of the film, sounds reasonable. In this context, Eq. (2.28) might be used as a semiempirical relation, ξ_1/κ_b being a fitting parameter. An analysis of the thickness dependence of the out-of-plane component of the dielectric constant in terms of Eq. (2.28), performed by Vendik and Zubko²⁴ for (Ba,Sr)TiO₃ thin films, yields values of ξ_1/κ_b in the range of 0.2–2.5 Å. Two examples of the experimental data on the thickness dependence of the out-of-plane permittivity of (Ba,Sr)TiO₃ thin films, which can be successfully fitted to Eq. (2.28), are shown in Fig. 6, in both cases ξ_1/κ_b being about 0.5 Å.

One more useful qualitative conclusion can be drawn on the basis of the above modeling for the out-of-plane component of the permittivity. Namely, its thickness dependence may be sensitive to the electrode material since the effective thickness of the surface dead layer is a function of the boundary conditions at the electrodes, which in turn may be dependent on the electrode material. Here, two hypotheses

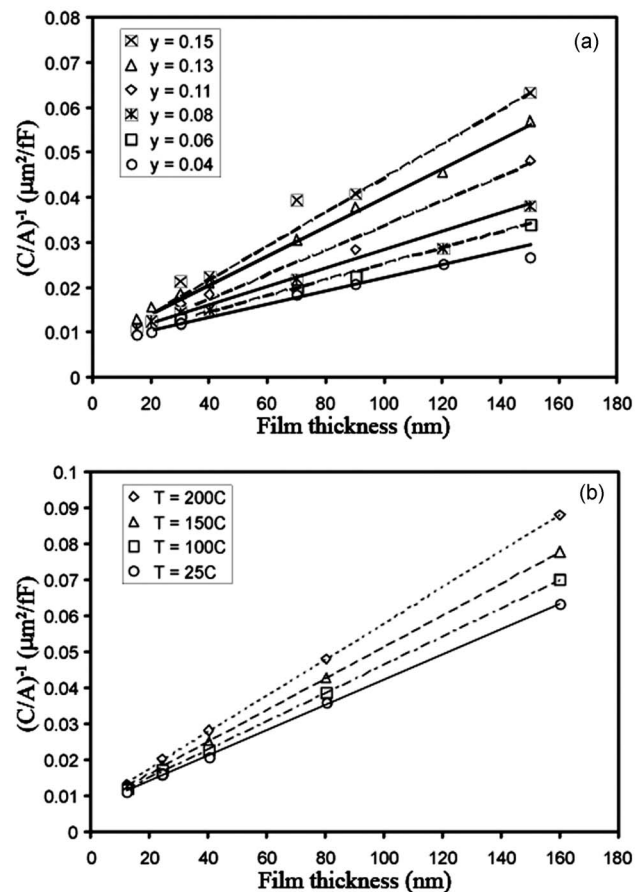


FIG. 6. (a) Film thickness dependences of the inverse zero-bias capacitance density of $(\text{Ba}_{0.7}\text{Sr}_{0.3})\text{Ti}_{1+y}\text{O}_{3+z}$ film based plate capacitors at different Ti content y (Ref. 25). (b) The inverse of the zero-bias capacitance density of $\text{Ba}_{0.7}\text{Sr}_{0.3}\text{TiO}_3$ film based plate capacitors as a function of film thickness at different temperatures (Ref. 26).

for the relation between the boundary condition in question and the electrode material should be mentioned. First, it has been suggested that the surface blocking of polarization is much less pronounced in the case of a similarity between the ferroelectric and electrode, specifically, when the electrode is oxide and the ferroelectric is an oxide perovskite.²⁷ The second hypothesis is that, in the case of an oxide electrode, the effective surface passive layer is short-circuited.¹⁰ Thus, both hypotheses imply that ferroelectric capacitors with oxide electrodes are expected to exhibit a weaker thickness dependence of the measured dielectric constant compared to those with metallic electrodes. According to Vendik and Zubko this trend is compatible with the existing experimental data.²⁷

Unlike the surface polarization blocking scenario, the mechanism related to the free charge distribution in the electrodes stands on more solid grounds. The prediction of this mechanisms, Eq. (2.18), which is strictly justified mathematically, is identical to the result for the out-of-plane permittivity of the ferroelectric-dielectric sandwich, with $d/\kappa_d = 2l_s$. Experimental data²⁴ for $(\text{Ba,Sr})\text{TiO}_3$ thin films place $d/2\kappa_d$ in the range of 0.2–2.5 Å, which is comparable to typical values of the Thomas-Fermi screening length, $l_s \approx 0.5$ Å.

A very important phenomenon hidden in Eqs. (2.16), (2.18), and (2.28), and, as we shall see later, (3.15) and

(3.16), is the shift of the Curie-Weiss temperature of the phase transition (i.e., the temperature at which the paraelectric phase becomes absolutely unstable). According to the Landau-Devonshire theory, the parameter α is a linear function of temperature, $\alpha = (T - T_0)/\varepsilon_0 C$, where C is the Curie-Weiss constant of the material and T_0 its Curie-Weiss temperature. In bulk ferroelectrics, we observe an anomaly of the permittivity $\kappa = 1/\alpha\varepsilon_0$ (when approaching the phase transition), which is used to identify the phase transition itself. In thin films, as we have just seen, the parameter $\alpha = 1/\kappa\varepsilon_0$ is affected by the presence of the passive layers—see Eqs. (2.16), (2.18), and (2.28)—via a renormalization of its value

$$\tilde{\alpha} = \alpha + \frac{d}{h\varepsilon_0\kappa_d}. \quad (2.31)$$

Therefore, the Curie-Weiss temperature T_0 is shifted down, $T_0 - \Delta T$, where

$$\Delta T = C \frac{d}{h\kappa_d}. \quad (2.32)$$

In this context, it is of interest to make a link between the phenomenological model discussed in this section and the recent results of *ab initio* calculations by Junquera and Ghosez for $\text{SrRuO}_3/\text{BaTiO}_3/\text{SrRuO}_3$ short-circuited sandwiches on SrTiO_3 substrates.²⁸ In this work, it has been found that the minimal thickness of the ferroelectric, at which it can bear a spontaneous polarization, is 24 Å. It follows that, at a thickness of around 24 Å, the transition temperature is the absolute zero. In other words, the depolarizing effect has lead to some 1300 K reduction of the transition and Curie-Weiss temperatures ($T_C \approx 1300$ K is the transition temperature of bulk BaTiO_3 , subject to an $\sim 2\%$ misfit strain due to the compressive action of the SrTiO_3 substrate²⁹). Taking for BaTiO_3 the value $C = 1.5 \times 10^5$ K from Eq. (2.32) we obtain $d/2\kappa_d \approx 0.1$ Å. This is smaller than the typical values of this parameter for systems with Pt electrodes discussed above. At the same time, the small value of this parameter is qualitatively consistent with smaller depolarizing effects observed in capacitors with oxide electrodes.²⁷

To conclude the discussion of passive layer effects, it is instructive to list the thicknesses of dielectric layers with $\kappa_d = 1$, producing the same effect as each of the passive layer mechanisms considered in this paper (see Table I).

D. Passive layer and domain contribution to dielectric permittivity

The extrinsic (domain) contribution to the dielectric permittivity of a ferroelectric thin film may be affected by electrostatic effects. This happens when the electric field in the film is not fully controlled by the potential difference between the electrodes of the capacitor, V , but also is sensitive to variations of the domain pattern. This situation readily occurs when the ferroelectric capacitor contains a passive nearby-electrode layer, so that the field in the ferroelectric differs from the applied one by the value of the depolarizing field. A simple and general approach to this problem is to consider the ferroelectric and the passive layer as two capaci-

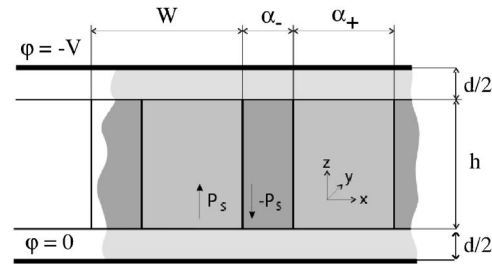


FIG. 7. Dense domain pattern in a ferroelectric capacitor system with passive nearby-electrode layers. W is the period of the domain pattern, α_+ (α_-) is the width of the positive (negative) domains, ϕ is the electric potential, and P_s is the spontaneous polarization from Landau-Devonshire theory.

tors connected in series. In Sec. II C, this approach was applied to the analysis of switching. Though simple and physically transparent, this approach is limited since it deals with values of the electric field and polarization averaged over the capacitor area. This description may not be adequate when the ferroelectric film contains an array of domains crossing the film from one electrode to the other (so-called through domains). An adequate description of this system requires taking into account not only the aforementioned average values of the electrical variables but also their stray components. In the framework of the theory of equilibrium domain pattern in a ferroelectric capacitor containing passive nearby-electrode layers and an array of “through” 180° domains (Fig. 7), the energy of stray electric fields can play a significant role. As was shown by Kopal *et al.*³⁰ and Bratkovsky and Levanyuk,^{31,32} stray fields also play a significant role in the small signal dielectric response of this system, so that the simple in-series capacitor approach may readily fail in its original formulation. However, further analysis of the problem by Mokry *et al.*³³ showed that, for a typical experimental situation of dense domain patterns and finite wall mobility, the in-series capacitor formula remains valid, though with a modified value (i.e., different from the real value of the material) of the permittivity of the passive layer. Let us consider the linear dielectric response of the aforementioned passive layer system (cf. Fig. 7). Specifically, following Mokry *et al.*³³ we will address the situation of a nonpoled domain pattern of period W , which, however, may be different from its equilibrium value. This is a reasonable approximation to a realistic situation for the system, since reaching the equilibrium domain configuration can easily be impeded by coupling of domains with crystalline defects in the ferroelectric. The out-of-plane component of the permittivity of the ferroelectric itself, $\kappa = \kappa_m + \kappa_c$, is taken as the sum of the intrinsic lattice contribution, κ_c , and the extrinsic one, κ_m , associated with the domain wall motion controlled by coupling between the walls and crystalline defects (defect pinning). In a capacitor containing the ferroelectric and passive layers, there are three factors that govern the linear dielectric response: (i) the rigidity of the crystalline lattice, which controls the intrinsic contribution κ_c ; (ii) the electrostatic energy of system; and (iii) the coupling of the domain walls with the imperfections of the system, which controls the extrinsic contribution κ_m . In terms of the thermodynamic potential, the description of the linear response requires consideration only of terms lin-

ear and quadratic in the net spontaneous polarization of the ferroelectric, $P_N \equiv (\alpha_+ - \alpha_-)P_s/W$ (Fig. 7). The part of this potential related to the electrostatic energy of the system can be written as³³

$$G_{el}/S = h \left[\frac{P_N^2}{2\varepsilon_0\kappa_{el}} - \frac{P_N V/h}{1 + \kappa_c d/(\kappa_d h)} \right], \quad (2.33)$$

where

$$\frac{1}{\kappa_{el}} = \frac{d}{\kappa_d h + \kappa_c d} + \frac{2W}{\pi h} \sum_{n=1}^{\infty} \frac{(-1)^n}{n D_n}, \quad (2.34)$$

$$D_n \equiv \kappa_d \coth\left(\frac{n\pi d}{W}\right) + \sqrt{\kappa_a \kappa_c} \coth\left(\sqrt{\frac{\kappa_a}{\kappa_c}} \frac{n\pi h}{W}\right),$$

with κ_a , κ_c , and κ_d being the in-plane and out-of-plane lattice permittivities of the ferroelectric and that of the passive layer, respectively. The parameter $1/\kappa_{el}$ has the meaning of the contribution to the inverse dielectric susceptibility of the system, which is controlled by the electrostatic energy of the domain pattern. The part related to the domain pinning by defects can be written as

$$G_m/S = \frac{h P_N^2}{2\varepsilon_0 \kappa_m}, \quad (2.35)$$

where κ_m is the extrinsic contribution to the permittivity of the ferroelectric introduced above. So if the ferroelectric with a given period of the domain pattern were placed in a passive-layer-free capacitor, the permittivity $\kappa = \kappa_m + \kappa_c$ would be measured. For the total thermodynamic potential of the system we therefore have

$$G_{tot}/S = h \left[\frac{P_N^2}{2\varepsilon_0 \kappa_w} - \frac{P_N V/h}{1 + \kappa_c d/(\kappa_d h)} \right], \quad (2.36)$$

where $1/\kappa_w = 1/\kappa_{el} + 1/\kappa_m$.

The response of the net spontaneous polarization P_N to the voltage V applied to the capacitor can be found from the condition for the minimum of the thermodynamic potential G_{tot} :

$$\partial G_{tot}/\partial P_N = 0. \quad (2.37)$$

The validity of Eq. (2.35) can be readily verified. Setting $d \rightarrow 0$ in Eqs. (2.34) and (2.36), from Eqs. (2.36) and (2.37) we get $P_N = \varepsilon_0 \kappa_m V/h$, in accordance with the definition of κ_m .

To calculate the effective permittivity of the system, $\kappa_{eff} \equiv C(h+d)/\varepsilon_0 S$, where C is its capacitance, Eqs. (2.33)–(2.37) should be appended with the relation

$$C/S = \frac{P_N/U + \varepsilon_0 \kappa_c}{1 + \kappa_c d/(\kappa_d h)}, \quad (2.38)$$

which can be obtained from the Poisson equation.^{30,32} Finally, Eqs. (2.33)–(2.38) yield³³

$$\frac{h+d}{\kappa_{eff}} = \frac{h}{\kappa_c + \kappa_w} + \frac{d}{\kappa_d} \left[1 - \left(\frac{\kappa_w}{\kappa_c + \kappa_w} \right)^2 \frac{h}{h+h_c} \right], \quad (2.39)$$

where $h_c = d\kappa_c^2/\kappa_w(\kappa_c + \kappa_w)$. Though formula (2.39) is similar to the in-series capacitor formula given by Eq. (2.14), the contribution of domain wall motion to the dielectric response

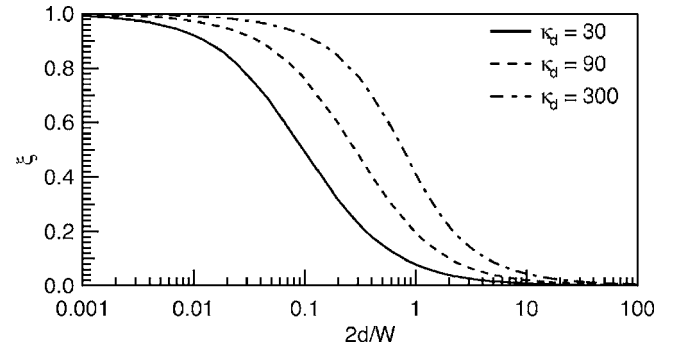


FIG. 8. The function $\xi(2d/W)$ appearing in Eq. (2.41), for three different values of the passive layer permittivity κ_d . When the passive layer thickness d is much greater than the domain pattern period W , the dense pattern approximation (2.40) reduces to the simple in-series capacitor formula (2.14). After Ref. 33.

of the system, κ_w , contains the function κ_{el} , which, in general, depends on the film thickness. Thus, in general, Eq. (2.39) exhibits a thickness dependence of the effective permittivity qualitatively different from that of the in-series capacitor formula. However, in the case of practical interest, where the domain pattern is dense ($W < h$) and the passive layer is thin ($d < h$), this relation can be simplified down to the following form,³³ which we will refer below as *dense pattern approximation*:

$$\frac{S\varepsilon_0}{C} \equiv \frac{h+d}{\kappa_{eff}} = \frac{h}{\kappa} + \frac{d}{\kappa_{mod}}, \quad (2.40)$$

where

$$\kappa_{mod} = \frac{\kappa_d}{1 - (\kappa_m/\kappa)^2 \xi(d/W)}, \quad (2.41)$$

$$\xi(\tau) = \frac{2\kappa_d}{\pi\tau} \sum_{n=1}^{\infty} \frac{(-1)^n/n}{\kappa_d \coth(n\pi\tau) + \sqrt{\kappa_c \kappa_a}}.$$

Here, $\xi(\tau)$ is a function decreasing from 1 to 0 with increasing τ . The plots of this function for three sets of parameters of the problem are shown in Fig. 8. Thus, one arrives at the in-series capacitor formula, Eq. (2.14), where, however, the real value of the passive layer permittivity, κ_d , is replaced by the apparent value κ_{mod} . The physical reason for this simplification is the following. In the case of a dense domain pattern, the stray fields created by the periodic charge distribution at one electrode essentially decay with the distance from this electrode. For this reason, the distribution of the electric field in the vicinity of an electrode (closer to the electrode than W) can be associated with a capacitor whose capacitance is independent of film thickness. Thus, the film behaves as a ferroelectric capacitor, corresponding to the bulk of the film connected in series with two capacitors which are associated with the distribution of the electric field in the vicinity of the electrodes.

Comparing the obtained result, Eq. (2.40), to the simple in-series formula, Eq. (2.14), we see that though the slope of the h dependence of the inverse capacitance is the same (the permittivity of the ferroelectric itself), in the polydomain case the offset of this dependence brings information not

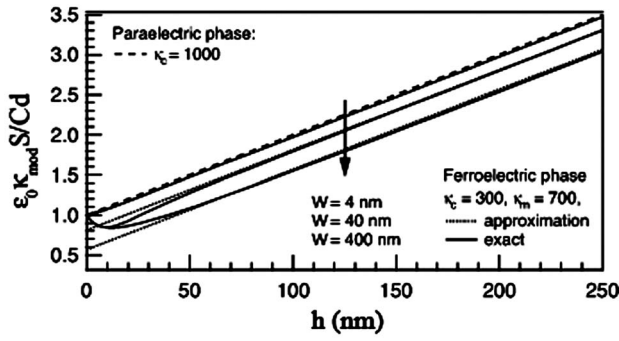


FIG. 9. Effect of domain spacing W on the offset of the film thickness (h) dependence of the normalized inverse capacitance, $\varepsilon_0\kappa_{\text{mod}}S/Cd$. The dashed line corresponds to the simple in-series capacitor formula, Eq. (2.14), the dotted lines to the dense pattern approximation, Eq. (2.40), and the continuous lines to the exact formula, Eq. (2.39). After Ref. 33.

only on the permittivity of the passive layer κ_d but also on the period of the domain pattern and the distribution of the dielectric response of the ferroelectric material itself between the intrinsic, κ_c , and extrinsic, κ_m , contributions.

The effect of domain spacing on the offset of the h dependence of the inverse capacitance predicted by Eq. (2.40) is illustrated in Fig. 9. It is seen that, in the polydomain case, this offset can be substantially smaller than that predicted by the simple in-series formula (shown with a dashed line). In this figure, the predictions of the dense pattern approximation, Eq. (2.40), are compared to those of the exact formula, Eq. (2.39). We see that, for dense domain patterns, i.e., for $h > W$, the former provides a very good approximation.

The sensitivity of the extrapolated offset of the h dependence of the inverse capacitance to the distribution of the dielectric response of the ferroelectric material between the extrinsic and intrinsic contributions is illustrated in Fig. 10. It is seen that the effect can be appreciable.

Two qualitative predictions following from the results obtained above are worth mentioning. First, since $\xi(d/W) \rightarrow 0$ as $d/W \rightarrow \infty$, in the limit of a thick passive layer, $d \ll W$, the dense pattern approximation, Eq. (2.40), reduces to the simple in-series capacitor formula with the true permit-

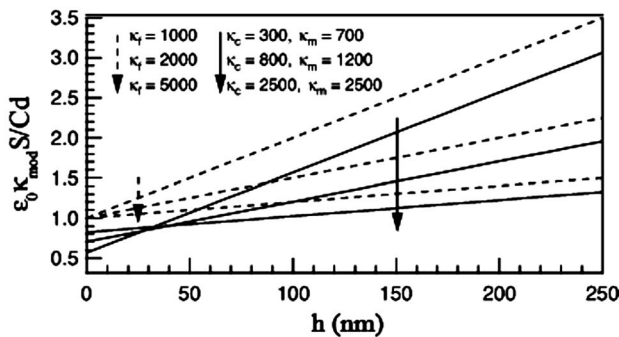


FIG. 10. The graph shows how the offset of the h dependence of $\varepsilon_0\kappa_{\text{mod}}S/Cd$ is affected by the distribution of the dielectric response ($\kappa = \kappa_c + \kappa_m$) of the ferroelectric system between the intrinsic (κ_c) and extrinsic (κ_m) contributions, for a dense domain pattern ($W=4$ nm). As in Fig. 9, the dashed line corresponds to the in-series capacitor formula, Eq. (2.14), while the continuous line to the dense pattern approximation, Eq. (2.39). After Ref. 34.

tivity of the passive layer, Eq. (2.14), disregarding the other parameters of the system. For the special case of infinite domain wall mobility, i.e., in the limit $\kappa_m \rightarrow \infty$ (so that $\kappa \rightarrow \infty$), this result reduces to the relation $\varepsilon_0S/C = d/\kappa_d$ derived earlier by Kopal *et al.*³⁰ and by Bratkovsky and Levanyuk.³²

The second prediction relates to the situation where the domain spacing significantly exceeds the thickness of the passive layer, i.e., $W \gg d$. In this case, $\xi(d/W) \rightarrow 1$, so that Eqs. (2.40) and (2.41) can be simplified as

$$\frac{h+d}{\kappa_{\text{eff}}} = \frac{h}{\kappa} + \frac{d}{\kappa_d} \left[1 - \frac{\kappa_m^2}{(\kappa_c + \kappa_m)^2} \right]. \quad (2.42)$$

Clearly, in this case the “suppressive” effect of the passive layer is drastically weakened when the dielectric response is dominated by the extrinsic contribution—i.e., $\kappa_m \gg \kappa_c$, so that $\kappa_m/(\kappa_m + \kappa_c) \rightarrow 1$. One explains this phenomenon as follows. At $W \gg d$, the stray fields in the passive layer at opposite domains differ only by their sign, except for small regions close to the domain walls, disregarding the displacements of the walls. This makes the energy density of these fields at the opposite domains equal to within $d/W \rightarrow 0$. This implies a significant reduction of the suppressive effect of the passive layers, an effect driven by the difference in these energy densities. Numerical simulations illustrating this effect for the case $\kappa_m/(\kappa_m + \kappa_c) = 1$ can be found in Ref. 32.

A prediction of the theory that can be checked experimentally is the temperature dependence of the extrapolated offset of the $S\varepsilon_0/C$ vs h dependence. Namely, in films where the dielectric data in the paraelectric phase suggest the presence of a passive layer, this offset in the ferroelectric phase may be essentially temperature dependent due to the expected temperature dependence of the ratio κ_m/κ_c . According to Mokry *et al.*,³³ the dielectric behavior of thin films of ferroelectric copolymer of vinylidene fluoride and tetrafluoroethylene might be explained in terms of this scenario.

The model discussed above has practical significance: on one hand, it shows the possibility of justifying the classical in-series formula for the case of films with dense domain patterns—though with an effective permittivity of the passive layer; on the other hand, it reveals some nontrivial features of the system, such as the reduced suppressive action of the passive layer on the extrinsic contribution to the permittivity. At the same time, when using the results provided by this model one should recognize its limitations. Among these, the most important seems to be the fact that the possibility of domain wall bending and the possible impact of charge transport across the passive layer have been neglected.

E. Imprint and passive layer

Very often the switching characteristics of ferroelectric thin film capacitors are not symmetric with respect to the reversal of the applied voltage. In this case, one speaks about the presence of an *internal bias field* in the capacitor to account for the asymmetry. Although writing the electric field seen by the ferroelectric as the sum of the applied and internal bias field does not usually correspond to a real situation

(as will become clear from the following discussion), we will be using the established term “internal bias” when speaking about the switching asymmetry—bearing in mind the ratio V_{off}/h , where V_{off} is the voltage offset of the switching characteristics of the film, and h is its thickness.

By the term “internal bias field effects” we mean two classes of phenomena: (i) *built-in internal bias field* development as a result of processing, and (ii) internal bias field development in the ferroelectric capacitor as a result of maintaining the capacitor in a poled state for some time (exposition time). The latter effect is customarily called *imprint*. During the exposition time the capacitor can also be treated with an electrical field, elevated temperature, or visible/UV light illumination. In the latter two situations one also uses the terms *thermal* and *optical imprint*, respectively.

In this subsection, we first theoretically address the relation between the amount of trapped charge and the parameters characterizing the switching asymmetry, following Ref. 35. Then based on this relation we consider the imprint scenario related to nearby-electrode charge transport.

1. Voltage offset caused by nearby-electrode trapped charge

It is obvious that space charge asymmetrically trapped (i.e., immobile on the time scale of the switching experiment) in the film should lead to some asymmetry of the ferroelectric switching. Typically, in thin films this charge is trapped nearby the ferroelectric-electrode interfaces. In this case, the ferroelectric capacitor can be roughly modeled as the in-series connection of an ideal ferroelectric capacitor and of another capacitor, having the thickness equal to the distance between the centroid of the trapped charge and the electrode, and having the charge equal to the total trapped charge sitting between the two capacitors. If we assume that due to the impact of the ferroelectric-electrode interface the latter (“surface”) capacitor is nonswitchable, we arrive at a simple model for the internal bias field effect driven by the electric charge trapped between the “ferroelectric” and surface capacitors. This model (where, in addition, the “material” of the surface capacitance is assumed to be nonpolar) has been used by Grossmann *et al.*^{36,37} and Tagantsev *et al.*³⁵ for the description of the imprint phenomenon. An electrostatically identical model has already been discussed in Sec. II B. This model contains a sandwich structure with a ferroelectric layer and a thin dielectric layer (passive layer) separated by the interface containing the trapped charge (see Fig. 1). The internal bias effect in this model is controlled by the relation between the voltage offset and the amount of trapped charge. To obtain this relation, one starts from the equations for the total voltage drop across the system and from the continuity of the displacement field:

$$V = hE_f + dE_d, \quad (2.43)$$

$$D_f - \sigma = \varepsilon_0 \kappa_d E_d, \quad (2.44)$$

whereby

$$D_f - \sigma = \varepsilon_0 \kappa_d \left(\frac{V}{d} - \frac{h}{d} E_f \right), \quad (2.45)$$

with V being the voltage applied to the capacitor; D_f and E_f the displacement and electric field in the ferroelectric, and h its thickness; E_d , d , and κ_d the field in the passive layer, its thickness, and its dielectric permittivity, respectively. Here, σ stands for the surface density of trapped charge at the ferroelectric-passive layer interface.

We define the voltage offset V_{off} as the difference in the applied voltages that produce the same switching in the cases of the charged and uncharged ferroelectric-passive layer interfaces. In terms of Eq. (2.45), “to produce the same switching” means to arrive at the same D_f and E_f . Following this definition and writing Eq. (2.45) for the capacitors with and without trapped charge, we find from the difference between these two equations:

$$V_{\text{off}} = - \frac{d\sigma}{\varepsilon_0 \kappa_d}. \quad (2.46)$$

It is instructive to rewrite Eq. (2.45) in terms of V_{off} and of the voltage applied to the ferroelectric layer, $V_f = hE_f$:

$$V_f = V - V_{\text{off}} + \frac{dD_f}{\varepsilon_0 \kappa_d}. \quad (2.47)$$

This equation clearly explains the statement at the beginning of Sec. II E: the electric field seen by the ferroelectric is not simply the sum of the applied and the internal bias field.

At this point it is important to mention that, in general, the voltage offset just calculated, V_{off} , may essentially differ from the voltage offset defined as the half-sum of the coercive voltages of the P - E loop of the same capacitor, $V_{\text{off-cr}}$. There are two reasons for that. First, if the ferroelectric loop is not saturated, in the presence of the internal bias the degree of saturation at the tips of the loop is different from that observed in the absence of the internal bias. For this reason, the switching curves of the ferroelectric, $D_f(E_f)$, may not be the same for these two cases. Hence Eq. (2.45) may no more lead to Eq. (2.46). Second, the measured P - E loops are usually symmetrized with respect to the P axis; therefore, in order to be compared with experimental data, the calculated loops should also be symmetrized by introducing some polarization offset. This polarization offset will result in an additional voltage offset.

It is instructive to write down the difference between $V_{\text{off-cr}}$ and V_{off} . In general, this is a complicated task. To give an idea about this effect, we will evaluate $V_{\text{off-cr}}$ within the present model for the case of saturated P - E loops in the so-called “hard ferroelectric” approximation, where it is set to

$$D_f = P_N + \varepsilon_0 \kappa_f E_f. \quad (2.48)$$

Here, P_N and κ_f are the domain part of polarization of the ferroelectric and the lattice contribution to its permittivity, respectively. In addition, close to the coercivity, we approximate the hysteresis loop of the ferroelectric as

$$D_f = \varepsilon_0 \kappa_{cr}(E_f - E_c), \quad (2.49)$$

where E_c is the coercive field of the ferroelectric and κ_{cr} is a constant controlling the slope of the loop at coercivity. Using Eq. (2.45) and the relation between the average displacement fields of the capacitor, D , and D_f —i.e.,

$$D = D_f - \sigma d / (h + d), \quad (2.50)$$

one readily finds for the polarization offset of the saturated loop (i.e., a loop with $P_N = \pm P_s$ at its tips):

$$\Delta D = \frac{d\sigma}{h} \left(\frac{\kappa_f}{\kappa_d^*} - \frac{h}{d+h} \right), \quad (2.51)$$

where

$$\kappa_d^* = \kappa_d + \frac{d}{h} \kappa_f. \quad (2.52)$$

(Once again, we have neglected the difference between the polarization and the displacement field in the ferroelectric system.) Using the relations above, one finds the values of the positive and negative coercive voltages of the symmetrized loop, V_+ and V_- , i.e., the values of the applied voltage at which the displacement field of the system equals ΔD :

$$V_{\pm} = \pm hE_c + \left(\frac{h}{\kappa_{cr}} + \frac{d}{\kappa_d} \right) \left(\Delta D + \frac{\sigma d}{d+h} \right) - \frac{d\sigma}{\kappa_d}. \quad (2.53)$$

This leads to the final expression for the voltage offset of the symmetrized loop:

$$\begin{aligned} V_{\text{off-cr}} &\equiv \frac{V_+ + V_-}{2} = - \frac{d\sigma}{\varepsilon_0 \kappa_d^*} \left(1 - \frac{\kappa_f}{\kappa_{cor}} \right) \\ &= V_{\text{off}} \frac{1 - (\kappa_f/\kappa_{cr})}{1 + (d\kappa_f/h\kappa_d)}. \end{aligned} \quad (2.54)$$

Relation (2.54) suggests that $V_{\text{off-cr}}$ and V_{off} may differ significantly. In the case of a ferroelectric material with square loops (i.e., where $\kappa_f \ll \kappa_{cr}$) and for very thin passive layers ($d \ll h\kappa_d/\kappa_f$), $V_{\text{off-cr}} \approx V_{\text{off}}$. On the other hand, for thicker passive layers ($d \gtrsim h\kappa_d/\kappa_f$), $V_{\text{off-cr}}$ and V_{off} can differ dramatically in value as well as in their functional dependence on the parameters of the problem. For instance, in the latter regime, V_{off} is independent of film thickness, whereas $V_{\text{off-cr}}$ is strongly dependent upon it.

2. Nearby-electrode injection model for imprint

The above consideration shows that when interpreting experimental data on the internal field effect, one should pay proper attention to the evaluation method for the internal bias. In thin ferroelectric films, as we have seen, the presence of nearby-electrode passive layers may be essential for various properties of the film. In the description of the impact of such a layer on ferroelectric domain patterns, on the coercive field of hysteresis loops, and on their tilt, the passive layer has been modeled as a thin dielectric layer between the ferroelectric and the electrode. A version of this model, which makes allowance for charge transport across the layer, is an appropriate mechanism also for the internal field effect. Grossmann *et al.*^{36,37} offered an imprint mechanism of this

kind for ferroelectric thin film capacitors. The driving force of the mechanism can be explained as follows. In a capacitor with such a passive layer, at remanence (i.e., when the capacitor is poled and then short-circuited), the bound charge of the remanent polarization is separated from the charge on the electrodes, and as a result the layer is subjected to a very high electric field (see the beginning of Sec. II B for an estimate). This field can promote charge transfer from the electrode to the ferroelectric-passive layer interface. During further electrical cycling, the field in the passive layer will change its direction following the variation of polarization in the ferroelectric. Accordingly, the charge at the ferroelectric-dielectric interface will change in time, its evolution depending on the cycling regime. If the time elapsed while the capacitor is at remanence is comparable to the cycling period, we expect a periodical variation of this charge with a vanishing average value. This situation has been addressed in Sec. II B, where it has been shown that, in this regime, the loop remains symmetric. If, however, the time elapsed while the capacitor is at remanence is much greater than the cycling period, it is possible that the charge at the ferroelectric-dielectric interface is only slightly time dependent, having an appreciable average value over the cycling period. This occurs if the charge accumulated at the interface is too large to be removed by the field in the layer during half the cycling period. The electric charge thus accumulated at the ferroelectric-passive layer interface will lead to the appearance of an internal bias field, as described above in Sec. II E 1.

In this model, the description of imprint requires first the calculation of the accumulated charge, and second, finding the voltage offset by using the corresponding relations from Sec. II E 1. Under reasonable assumptions on the charge transport across the passive layer, one finds that the offset voltage is a logarithmic-type function of the time spent by the capacitor in the poled state (the “exposition time”), which agrees qualitatively with experimental observations (see the later discussion in Sec. V). This logarithmic-type time dependence of the voltage offset was demonstrated by Grossmann *et al.* using numerical simulation³⁷ and by Tagantsev *et al.*³⁵ using an analytical approach. We will now present the analytical approach.

First, we consider the situation where the capacitor is under open-circuit conditions during the exposition time. Depending on the parameters of the system, the electrical conditions may alter some of the conclusions of the analysis. We will return to this point later. In the model we are considering, the charge transport across the passive layer is fully described by Eqs. (2.43) and (2.44) and by the equation for the charge accumulation (2.10), where the hard ferroelectric approximation (2.48) is adopted as the constitutive equation of the ferroelectric. We consider the situation where, originally, the ferroelectric is not poled, i.e., $P_N = 0$, and where the charge at the ferroelectric-passive layer interface is equal to zero, i.e., $\sigma = 0$. Then the ferroelectric is poled with a voltage pulse (i.e., we set $P_N = P_s$ and $V = 0$ just after the application of the pulse) and left in this poled state. In the presence of the passive layer, the polarization of the ferroelectric will result in a depolarizing field in the ferroelectric film and in a

strong field in the passive layer. The high electric field in this layer will cause charge transport across it, resulting in the accumulation of charge σ . Let us calculate this charge, $\sigma(t, P_s)$, as a function of the exposition time, t , for the case of an open electric circuit. The condition $P_N = P_s$ is assumed to hold at any t , which corresponds to the situation where the polarization relaxation rate is smaller than the rate of charge accumulation at the interface. A proper variable for the calculations is the field in the passive layer, E_d , which satisfies the relations following from Eqs. (2.10), (2.43), (2.44), and (2.48):

$$\varepsilon_0 \kappa_d \frac{dE_d}{dt} = -J(E_d), \quad (2.55)$$

$$\sigma = -\kappa_d \varepsilon_0 [E_d(0) - E_d(t)], \quad (2.56)$$

$$E_d(0) = -\frac{P_s}{\varepsilon_0 \kappa_d}. \quad (2.57)$$

Equations (2.55) and (2.56) have been obtained using the open electric circuit conditions, which in the present model correspond to a time-independent electric displacement field in the ferroelectric; Eq. (2.57) corresponds to the condition $V=0$, which is valid just after the poling, i.e., at $t=0$. Equations (2.55)–(2.57), appended with the law for the charge transport across the passive layer, $J(E)$, specify the mathematical problem. We will consider the situation where the charge transport across the passive layer can be described by an exponential equation, i.e., where $J(E)$ can be written as

$$J(E) = A \left(\frac{E}{E_{th}} \right)^\alpha \exp \left[\operatorname{sgn} \beta \left(\frac{E}{E_{th}} \right)^\beta \right]. \quad (2.58)$$

This situation covers the Poole-Frenkel and the thermionic (Schottky) and cold-field emission mechanisms, which are typical for dielectrics at high electric fields.³⁸ By introducing the new variable³⁹

$$q = \exp \left[\operatorname{sgn} \beta \left(\frac{E_d}{E_{th}} \right)^\beta \right], \quad (2.59)$$

we can rewrite Eq. (2.55) as

$$\tau \frac{dq}{dt} = -|\ln q|^\gamma q^2, \quad (2.60)$$

where

$$\tau = \frac{\varepsilon_0 \kappa_d E_{th}}{|\beta| A} \quad \text{and} \quad \gamma = 1 + \frac{\alpha - 1}{\beta}. \quad (2.61)$$

In the so-called “weak screening” case, an approximate analytic solution to this equation is possible (this kind of solution is well known in the theory of transient currents in dielectrics—cf., e.g., Ref. 40). In this case, where the conduction in the passive layer is truly exponential (i.e., $1/|\ln q| \ll 1$), and the polarization screening by the trapped charge is far from saturation (i.e., the current value of σ is much smaller than its value at the end of screening, which for the open-circuit conditions equals $P_s \kappa_d / \kappa_d^*$), the solution to Eq. (2.60), to within the accuracy of small parameters $1/|\ln q|$ and $\kappa_d^* / \kappa_d \times \sigma / P_s$, can be presented as³⁵

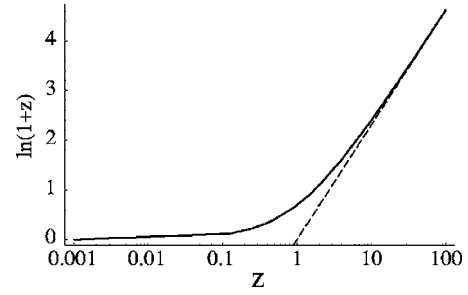


FIG. 11. Time dependence ($z=t/\tau_0$) of the voltage offset (V_{off}/V_0), in the case of weak compensation of the depolarizing field by carrier transport across the passive layer, Eq. (2.66).

$$\frac{q(0)}{q} = 1 + \frac{t}{\tau_0}, \quad (2.62)$$

where

$$\tau_0 = \frac{\tau}{q(0)|\ln q(0)|^\gamma}, \quad (2.63)$$

and the initial value of q is $q(0) = \exp[\operatorname{sgn} \beta (P_s / \kappa_d^* E_{th})^\beta]$. Using Eqs. (2.56), (2.57), (2.62), and (2.63) we find the accumulated charge as a function of the exposition time and of other parameters of the problem:

$$\sigma = \frac{\varepsilon_0 \kappa_d E_{th}}{|\beta|} \left(\frac{P_s}{\varepsilon_0 \kappa_d^* E_{th}} \right)^{1-\beta} \ln(1 + t/\tau_0), \quad (2.64)$$

where

$$\tau_0 = \frac{\kappa_d}{\kappa_d^*} \frac{P_s}{|\beta| A} \left(\frac{\varepsilon_0 \kappa_d^* E_{th}}{P_s} \right)^{\alpha+\beta} \exp \left[-\operatorname{sgn} \beta \left(\frac{P_s}{\varepsilon_0 \kappa_d^* E_{th}} \right)^\beta \right]. \quad (2.65)$$

According to Eq. (2.46), this leads to the following expression for the voltage offset:⁴¹

$$V_{\text{off}} = V_0 \ln(1 + t/\tau_0), \quad (2.66)$$

where

$$V_0 = \frac{dE_{th}}{|\beta|} \left(\frac{P_s}{\varepsilon_0 \kappa_d^* E_{th}} \right)^{1-\beta}. \quad (2.67)$$

We therefore see that the exponential form of the conduction equation for the passive layer leads to a universal logarithmic-type time dependence for the voltage offset, in the case of weak compensation of the depolarizing field by carrier transport across the passive layer. This dependence is illustrated in Fig. 11. The explicit expression for the voltage offset, Eq. (2.66), is controlled only by two parameters, V_0 and τ_0 , which have the meaning of the “logarithmic slope” in the regime of logarithmic charge relaxation and of the cross-over time between the regimes of linear and logarithmic relaxations, respectively. Equations (2.65) and (2.66), and the explicit expressions for the parameters entering these relations, enable us to extract some clear predictions from the theory.

Imprint is a logarithmic function of time only in the limit of large times. In general, it is not linear in the semilogarithmic scale. Its semilogarithmic dependence might give the

impression that the imprint accelerates with time. In reality, the relaxation slows down with time (sublinear), and its apparent acceleration is an artifact of the semilogarithmic scale.

Equations (2.65) and (2.66) lead to a description of the temperature dependence of the imprint in the case of the Poole-Frenkel mechanism, of thermoionic emission, and of cold-field emission.³⁸ In the case of thermoionic emission and of the Poole-Frenkel mechanism, $\beta=1/2$ and

$$E_{\text{th}} = \frac{4\pi\epsilon_0\kappa_h(k_B T)^2}{be^3}, \quad (2.68)$$

where κ_h is the optical dielectric constant of the material, T is the temperature, e is the charge of the electron, and $b=1$ for thermoionic emission and $1 < b < 2$ for the Poole-Frenkel mechanism. For these mechanisms, the parameter α may acquire the values of 1, $3/4$, and 0, depending on the field interval. The factor A from Eq. (2.58) is basically an exponential function of temperature:

$$A \propto \exp\left(-\frac{\Phi}{k_B T}\right), \quad (2.69)$$

where Φ stands for the Poole-Frenkel or the interfacial Schottky activation barrier.

Using the above relations, for the situation where the charge transport across the passive layer is controlled by the thermoionic or Poole-Frenkel mechanisms, we find

$$V_0 = 2d \sqrt{\frac{P_s E_{\text{th}}}{\epsilon_0 \kappa_d^*}} \propto dT \sqrt{\frac{P_s}{\kappa_d^*}}, \quad (2.70)$$

$$\ln \tau_0 = A_0 + \frac{\tilde{\Phi}}{k_B T}, \quad (2.71)$$

where A_0 is a weakly temperature-dependent constant and $\tilde{\Phi}$ is the activation barrier calculated with the field-induced reduction. From these relations and Eq. (2.66) we conclude that, in this case where the charge transport is thermally activated, the temperature dependence of the imprint is very different for the regimes of linear and logarithmic charge relaxations. In the linear regime—i.e., when $t \ll \tau_0$, the temperature dependence of $V_{\text{off}} \propto V_0/\tau_0$ is exponential, with the activation energy equal to that of the conduction mechanism responsible for charge transport across the passive layer. On the other hand, in the logarithmic regime—i.e., when $t \gg \tau_0$, the explicit temperature dependence of $V_{\text{off}} \propto V_0(\ln t - \ln \tau_0)$ is close to linear.

The results for the case of tunneling transport through the passive layer, where $\beta=-1$ and $\alpha=2$,³⁸ can be obtained on the same lines. However, in this case, $\gamma=0$ and Eq. (2.62) provides an exact solution to Eq. (2.60) for an arbitrary degree of polarization screening. For the accumulated charge this solution yields

$$\sigma = P_s \frac{\kappa_d}{\kappa_d^*} \frac{\ln(1 + t/\tau_0)}{\ln(1 + t/\tau_0) + \epsilon_0 \kappa_d^* E_{\text{th}}/P_s}. \quad (2.72)$$

In the case of weak screening, this relation is consistent with Eqs. (2.64)–(2.67). It clearly shows that the approximate solution is justified at $\sigma \ll \kappa_d/\kappa_d^* P_s$.

The above analysis has treated the case of charge relaxation under open electrical conditions for the external circuit. These conditions are consistent with the experimental situation at small times, since during the exposition time the capacitor is typically electrically disconnected from the rest of the circuit. However, at long enough times, the parasitic charge transport between the electrodes may become important, shifting the situation close to the short-circuited electrical conditions. For this reason, it is instructive to evaluate the impact of the electrical conditions on the charge relaxation. An analysis similar to that given above readily shows that, under short-circuited conditions, the basic equations (2.55) and (2.56) should be modified by the substitution of the permittivity of the passive layer, κ_d , with κ_d^* . The modified equations will still lead to Eq. (2.66), but Eqs. (2.65), (2.67), (2.70), and (2.72) should be replaced with their modified versions:

$$\tau_0 = \frac{P_s}{|\beta|A} \left(\frac{\epsilon_0 \kappa_d^* E_{\text{th}}}{P_s} \right)^{\alpha+\beta} \exp \left[- \left(\frac{P_s}{\epsilon_0 \kappa_d^* E_{\text{th}}} \right)^{\beta} \right], \quad (2.73)$$

$$V_0 = \frac{\kappa_d^* d E_{\text{th}}}{\kappa_d |\beta|} \left(\frac{P_s}{\epsilon_0 \kappa_d^* E_{\text{th}}} \right)^{1-\beta}, \quad (2.74)$$

$$V_0 = 2d \frac{\kappa_d^*}{\kappa_d} \sqrt{\frac{P_s E_{\text{th}}}{\epsilon_0 \kappa_d^*}} \propto dT \sqrt{P_s \kappa_d^*}, \quad (2.75)$$

$$\sigma = P_s \frac{\ln(1 + t/\tau_0)}{\ln(1 + t/\tau_0) + \epsilon_0 \kappa_d^* E_{\text{th}}/P_s}. \quad (2.76)$$

It is clear that these modifications will not affect the principal conclusions obtained above; however, there might be some changes in the details when κ_d and κ_d^* are essentially different—i.e., when $d\kappa_f \gg h\kappa_d$. For instance, in this case, $V_0 \propto \sqrt{hd}$ for the open-circuit situation, whereas $V_0 \propto \sqrt{d^3/h}$ under short-circuited conditions.

III. FERROELECTRIC-ELECTRODE CONTACT POTENTIAL PHENOMENA

A. Depletion-influenced switching

1. Depletion-assisted nucleation of reverse domains

The electrochemical interaction between the conductive electrodes and the electronic carriers of the ferroelectric may result in the so-called depletion effect, i.e., the removal of charge carriers from narrow nearby-electrode regions, whereby charged regions of bare impurities are formed close to the electrodes. In the case of a wide-gap and heavily compensated semiconductor, which is often the case for typical ferroelectrics, this built-in charge is related to deep trapping centers and oxygen vacancies.⁴² This charge can be considered as immobile during electrical measurements at room temperature and homogeneous inside the depletion layers.⁴³ The depletion phenomenon is characterized by the parameter W , the *depletion layer thickness*, which is a function of the electrochemical parameters of the ferroelectric-electrode interface:

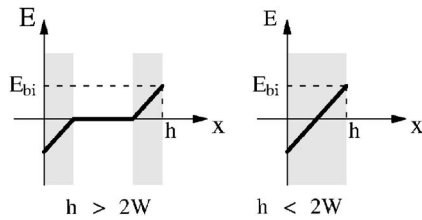


FIG. 12. Distribution of the built-in electric field in a film with depleted charge carriers, in the case of partial depletion ($h > 2W$) and of full depletion ($h < 2W$). The shaded areas correspond to the depleted regions of the film.

$$W = \sqrt{\frac{2\epsilon_0\kappa_l V_{bi}}{eN_d}}, \quad (3.1)$$

where e and N_d are the charge of the doping centers and their concentration, V_{bi} is the built-in potential, and κ_l is the lattice dielectric constant of the ferroelectric at the temperature at which electrochemical equilibrium is reached at the electrodes.⁴⁴ If the film thickness h is larger than $2W$, the film will contain two space-charged layers at the two electrodes and a neutral region in the middle. This is the case of *partial depletion*. If $h < 2W$, the film is homogeneously filled with space charge. This is the case of *full depletion*. A sketch of the built-in electric field distribution in a film with depleted charge carriers is shown in Fig. 12. The surface value E_{bi} of the built-in field created by the space charge can be found in the form (cf., e.g., Ref. 45)

$$E_{bi} = \frac{eN_d}{\epsilon_0\kappa_f} W \quad \text{for } h > 2W, \quad (3.2)$$

$$E_{bi} = \frac{eN_d h}{\epsilon_0\kappa_f 2} \quad \text{for } h < 2W.$$

In a real ferroelectric capacitor, one can assume for simplicity that the deposition or top-electrode annealing temperature is the temperature at which electrochemical equilibrium is reached.⁴⁶ Referring the reader to the original paper⁴⁵ for a more detailed discussion, we shall only outline the suggested mechanism for the thickness dependence of the coercive field E_c . Consider the switching from a negatively poled single-domain state when a positive external field E is applied to the capacitor. The first step of the switching is the nucleation of reverse domains. Since for $E > 0$ the total (depletion+external) field reaches its maximum at one of the electrodes (the one on the right in Fig. 12), the nucleation of positive domains will occur at this electrode. Let the nucleation threshold field be E_{cn} . The condition for surface nucleation can then be written as

$$E_{cn} = E + E_{bi}. \quad (3.3)$$

If the threshold field is much higher than the field required to maintain the domain walls (created due to the nucleation) in motion, then nucleation is the bottleneck of switching, and the condition for nucleation (3.3) is also the condition for switching. One can thus find the coercive field from Eqs. (3.2) and (3.3) as

$$E_c = E_{cn} - Ah, \quad A \equiv \frac{eN_d}{2\epsilon_0\kappa_f} \quad (h < 2W). \quad (3.4)$$

For thicker films, where the surface built-in field is thickness independent, one expects a thickness-independent coercive field.

This mechanism can explain the thickness dependence of the coercive field in PZT films with Pt electrodes thinner than a few micrometers. In this interval, a pronounced thickness dependence of E_c is documented for $h < h_d = 0.5 \mu\text{m}$, with a typical slope $A = \partial E_c / \partial h \approx (0.15-0.25) \times 10^7 \text{ kV/cm}^2$ (cf. Ref. 45). This corresponds to a concentration of once-ionized doping centers $N_d = 2A\kappa_f\epsilon_0/e \approx (0.3-0.4) \times 10^{19} \text{ cm}^{-3}$ ($\kappa_f = 300$ was used as an estimate). On the other hand, in terms of this model, the appearance of the thickness dependence of E_c at $h \approx h_d = 0.5 \mu\text{m}$ implies the depletion layer width in the bulk material, W , to be about $h_d/2 = 0.25 \mu\text{m}$. From the above values of W and A , and by using the relation $V_{bi} = AW^2$ [from Eq. (3.1) with $\kappa_l \approx \kappa_f$], the contact built-in potential can also be evaluated: $V_{bi} \approx 1 \text{ V}$. The estimates obtained for N_d , W , and V_{bi} are comparable with typical values of these parameters in perovskites.⁴⁷⁻⁴⁹ Hence, the suggested mechanism looks compatible with the semiconductor properties of perovskites.

2. Voltage offset due to the depletion effect

We have seen that semiconductor depletion may influence the switching behavior of ferroelectric thin films. The driving force of this phenomenon is the formation of nearby-electrode regions of immobile space charge which produces a built-in electric field. Of importance is that this built-in field does not vary during switching. In the case where the electrochemical states of the two nearby-electrode regions of the ferroelectric are not identical, an asymmetry in the switching process may occur. The relation between the asymmetry of the built-in electric field and that of the hysteresis loops is sensitive to the switching scenario. We will now discuss the case of the scenario addressed above in Sec. III A 1, where nearby-electrode nucleation of reverse domains is considered as the bottleneck of switching.

Let us start with the case of partial depletion. This is illustrated in Fig. 12 for the situation where the electrochemical states of the nearby-electrode regions of the ferroelectric are identical, so that the depletion regions have the same thickness. If this is not the case, e.g., if the surface built-in potentials are different for the two ferroelectric-electrode interfaces, the depletion widths at the two electrodes will be different. Along the same lines of the problem treated in Sec. III A 1, we can relate the surface built-in potentials V_1 and V_2 to the widths W_1 and W_2 of the depletion layers (the suffix refers to the particular electrode). This relation—from Eq. (3.1)—reads

$$V_1 = \frac{eN_d}{2\epsilon_0\kappa_l} W_1^2, \quad V_2 = \frac{eN_d}{2\epsilon_0\kappa_l} W_2^2. \quad (3.5)$$

From Eq. (3.2), the built-in fields at the electrodes are

$$E_1 = \frac{eN_d}{\varepsilon_0\kappa_f}W_1, \quad E_2 = -\frac{eN_d}{\varepsilon_0\kappa_f}W_2. \quad (3.6)$$

According to the model, switching takes place once the electric field seen by the ferroelectric at its interface with an electrode (sum of the applied and built-in fields) reaches a critical value of E_{c0} . Thus, the absolute values of both the coercive fields of the system will always be smaller than E_{c0} , namely, $E_{c0}-|E_1|$ and $E_{c0}-|E_2|$. Using Eqs. (3.5) and (3.6), we can evaluate the voltage offset of the polarization loop (nonsymmetrized along the P axis) via the half-sum of the coercive voltages. This half-sum gives

$$\begin{aligned} V_{\text{off}} &= -h \frac{\kappa_l E_{c0} - |E_1| - (E_{c0} - |E_2|)}{\kappa_f} \\ &= \frac{\kappa_l}{\kappa_f} (V_1 - V_2) \frac{h}{W_1 + W_2} \quad (h > W_1 + W_2). \end{aligned} \quad (3.7)$$

Here, the voltage offset is given for the case where the loop is monitored as a function of the potential difference between electrode “2” and electrode “1.”

The case of full depletion—i.e., where $h < W_1 + W_2$, can be treated similarly to obtain the following expression for the voltage offset:

$$V_{\text{off}} = \frac{\kappa_l}{\kappa_f} (V_1 - V_2) \quad (h < W_1 + W_2). \quad (3.8)$$

We thus see that the depletion effect may lead to a voltage offset in the polarization loop. In the case of full depletion, it is equal to the difference between the built-in potentials (which are responsible for the formation of depletion layers near the two electrodes) times the factor κ_l/κ_f . This extra factor arises from the fact that we do not expect electrochemical equilibrium at room temperature, while the built-in potentials form during processing at much higher temperatures. For films thicker than $W_1 + W_2$, partial depletion occurs, and the voltage offset becomes larger than $\kappa_l(V_1 - V_2)/\kappa_f$ and proportional to the film thickness. Considering that values in the range of 1–2 V are a realistic estimate for these potentials and that $\kappa_l \sim \kappa_f$, a voltage offset up to a few volts can be predicted by the depletion model. It is of interest to note that this model predicts a correlation between the thickness dependences of the coercive field (cf. Sec. III A 1) and of the “field offset” V_{off}/h : in the case of full depletion, both are thickness dependent, whereas they are thickness independent in the case of partial depletion.

It is instructive to consider the applicability of Eqs. (3.7) and (3.8). In general, the interfacial built-in potentials are fully controlled by the materials the ferroelectric and the electrode are made of. However, the potentials V_1 and V_2 introduced above can be identified with the aforementioned contact potentials with a reservation. Let us elucidate this issue for a situation often met experimentally. A ferroelectric film is deposited and crystallized onto a metallic bottom electrode (electrode 1) at a rather high temperature—e.g., 650°C. Then a top electrode of the same metal (electrode 2) is deposited at a much lower temperature—e.g., 200°C. Let the contact potential between the ferroelectric and the electrodes be V_0 . Formally, in this situation one might set V_1

$= V_2 = V_0$. In reality, the condition for the formation of depletion layers at the two electrodes is very different. Notably, one can expect that at 650°C electrochemical equilibrium (involving deep trapping levels) is reached at the electrode, whereas the temperature of 200°C might well not be high enough to reach this equilibrium. In such a situation, a depletion layer is formed only near the first electrode, so that according to the definition of V_1 and V_2 as *potentials* responsible for the formation of depletion layers in the capacitor, we should set $V_1 = V_0$ and $V_2 = 0$. We thus see that the difference between the contact potentials at the electrodes and the potentials V_1 and V_2 can be essential, and the model can predict a nonzero voltage offset in the case where the material of the two electrodes is the same.

B. Depletion-induced change of permittivity

The impact of the depletion effect on the polarization response of ferroelectric thin films was already discussed in Sec. III A 1, in the context of their switching behavior. In this subsection, we will address the impact of the built-in space charge induced by the depletion effect on the lattice contribution to the small signal polarization response of a ferroelectric film in the paraelectric phase. We will consider the cases of full and partial depletions illustrated in Fig. 12. We will show that, for the small signal response, the effect of depletion is similar to that of a passive surface layer. This result is consistent with that obtained by Bratkovsky and Levanyuk,⁵⁰ who treated the problem in the case of full depletion.

The impact of the depletion space charge on the effective dielectric permittivity of a parallel plate capacitor containing a ferroelectric can be elucidated through the following simple arguments.⁵¹ The built-in depletion charge results in a certain built-in electric field, which in turn creates a built-in, x -dependent polarization $P_{\text{bi}}(x)$, x being the coordinate normal to the plane of the film. For the dielectric response of the film, this implies a local x -dependent permittivity. Using the equation of state of the ferroelectric, $E = \alpha P + \beta P^3$, the out-of-plane component of the local permittivity can be written as

$$\kappa_{\text{loc}}(x) = \frac{1}{\varepsilon_0} \left(\frac{\partial E}{\partial P} \right)^{-1} \bigg|_{P=P_{\text{bi}}} = \frac{1}{\varepsilon_0} \frac{1}{\alpha + 3\beta P_{\text{bi}}^2(x)}. \quad (3.9)$$

Taking into account the in-series geometry of the problem, the effective dielectric constant of the system can be found by averaging $1/\kappa_{\text{loc}}(x)$ across the film thickness:

$$\frac{1}{\kappa_{\text{eff}}} = \frac{1}{h} \int_0^h \frac{dx}{\kappa_{\text{loc}}(x)} = \frac{1}{\kappa} + \frac{3\beta\varepsilon_0}{h} \int_0^h P_{\text{bi}}^2(x) dx, \quad (3.10)$$

where $\kappa = 1/\alpha$ is the lattice permittivity in the paraelectric phase. The exact value of $P_{\text{bi}}(x)$ can be obtained from a rather cumbersome solution to the equation of state for the ferroelectric and the Poisson equation:

$$\frac{d}{dx}[\varepsilon_0 \kappa_b E + P_{bi}(x)] = \rho(x), \quad (3.11)$$

where $\rho(x)$ is the built-in charge density and κ_b the background permittivity introduced in Sec. II C. This solution should also obey the condition

$$\int_0^h E dx = 0. \quad (3.12)$$

A good approximation for the built-in polarization can be readily obtained if, in Eq. (3.11), one neglects the term $\varepsilon_0 \kappa_b E$.⁵⁰ This approximation is justified by the large value of the dielectric permittivity of the ferroelectric ($\kappa \gg \kappa_b$). Then, Eqs. (3.11) and (3.12) yield

$$P_{bi}(x) = (x - h/2)\rho_0 \quad (3.13)$$

for the full depletion case (where $h < 2W$), and

$$P_{bi}(x) = (x - W)\rho_0 \quad \text{for } 0 < x < W, \\ P_{bi}(x) = 0 \quad \text{for } W < x < h - W, \quad (3.14)$$

$$P_{bi}(x) = (x - h + W)\rho_0 \quad \text{for } h - W < x < h,$$

for the case of partial depletion (where $h > 2W$). Here, W is the depletion layer width and $\rho_0 = eN_d$ the space charge density in the depleted regions, e and N_d being the charge and the volume density of ionized impurities in the depleted regions.

Using this result for the built-in polarization and Eq. (3.10), we find that depletion leads to a reduction of the effective dielectric permittivity of the film. In the cases of full and partial depletions, one finds⁵¹

$$\frac{1}{\kappa_{\text{eff}}} = \frac{1}{\kappa} + \frac{\varepsilon_0 \beta \rho_0^2 h^2}{4}, \quad (3.15)$$

and

$$\frac{1}{\kappa_{\text{eff}}} = \frac{1}{\kappa} + \frac{2\varepsilon_0 \beta \rho_0^2 W^3}{h}, \quad (3.16)$$

respectively. Equations (3.15) and (3.16) imply that, for the effective dielectric permittivity of the film, the depletion effect is equivalent to the in-series connection of the ferroelectric with a linear capacitor. In the case of partial depletion, this capacitance is independent of film thickness, so that the film behaves like a film with a real passive layer, while in the case of full depletion, according to Eq. (3.15), this capacitance goes as h^{-3} . A comparison of the passive layer effect due to depletion with other passive layer effects is presented in Table I.

It is instructive to evaluate the potential impact of depletion on permittivity. Numerically, it is not substantial; it is, however, comparable with that of the effective passive layers discussed in Sec. II C. For values of W and ρ_0 compatible with the data on ferroelectric perovskites with metallic electrodes ($W = 0.2 \mu\text{m}$, $\beta = 8 \times 10^9 \text{ J C}^{-4} \text{ m}^5$, and $\rho_0 \approx 0.16 \text{ C/cm}^3$, cf. Refs. 42, 45, 48, and 51) one finds that, in the case of partial depletion (where $h > 2W$), a single depletion layer works as a dielectric layer with $\kappa_d = 1$ and thickness

TABLE I. Thickness of a dielectric layer with $\kappa_d = 1$, which affects the dielectric permittivity of the film identically to the effects listed in the first column. h —film thickness, d —thickness of the layer, ξ —correlation radius, κ and κ_b —permittivity and background permittivity of the ferroelectric, λ —extrapolation length for the polarization boundary conditions, l_s —Thomas-Fermi screening length, β —coefficient of the dielectric nonlinearity, ρ_0 —space charge density in the depletion layer, and W —depletion layer width.

Effect	In-plane permittivity	Out-of-plane permittivity
Real layer with $\varepsilon_d = 1$	d	d
Full surface blocking of polarization	ξ	$\xi_1 / \kappa_b = \xi / \sqrt{\kappa \kappa_b}$
Partial surface blocking of polarization	$\xi / (1 + \lambda / \xi)$	$(\xi_1 / \kappa_b) / (1 + \lambda / \xi_1)$
Electrode effect	...	l_s
Partial depletion effect, $h > 2W$...	$h_d = \varepsilon_0 \beta \rho_0^2 W^3$
Full depletion effect, $h < 2W$...	$h_d (h/2W)^3$

$h_d = \varepsilon_0 \beta \rho_0^2 W^3 \approx 0.15 \text{ \AA}$. In the case of full depletion, the effect of depletion on permittivity can be identified with a strong reduction of the effect with decreasing film thickness—cf. Eq. (3.15). It is also worth mentioning that, as for any “in-series model,” the impact of depletion on the dielectric constant of a ferroelectric material in the paraelectric phase is formally equivalent to a lowering of its Curie-Weiss temperature.⁵⁰

IV. POLING EFFECT OF THE INTERFACE

A. Internal bias and misfit dislocations

A possible source of internal bias in ferroelectric thin film capacitors is the mechanical coupling between the ferroelectric material and the electrodes. Internal bias occurs when the atomic structure of the interface between the ferroelectric and the electrode favors a certain direction of polarization in the capacitor. In this section we will discuss a simple scenario for such effect, which is related to dislocation-assisted stress release in epitaxial films.

In epitaxial films at the ferroelectric-substrate (bottom electrode) interface, the lattice of the ferroelectric has to perfectly match that of the substrate, while the bulk lattice constants of the two materials are different. It follows that, at the interface, the ferroelectric is always strained. Typically, this strain leads to the appearance of misfit dislocations,⁵² and as a result the strain decays with the distance from the interface, creating a strain gradient. This strain gradient induces a linear polarization response via the flexoelectric effect (see, e.g., Refs. 53–56). However, in contrast to the piezoelectric effect, the flexoelectric effect can control the sign of the ferroelectric polarization (poling effect). If this poling effect is large enough, an internal bias can appear in the capacitor. Let us evaluate the magnitude of this poling effect and the corresponding voltage offset.

Let the value of the in-plane lattice constant of the unstrained ferroelectric be a and that of the ferroelectric in the vicinity of the ferroelectric-substrate interface be $a_s > a$. In the case of cube-on-cube ferroelectric-substrate epitaxy, a_s is just the lattice parameter of the substrate (bottom electrode). The lattice constant of the ferroelectric in the bulk of the film, a_s^* , which lies between a and a_s , is controlled by the

density of misfit dislocations at the ferroelectric-substrate (bottom electrode), ρ . For simplicity, we consider the case where the Burgers vector lies in the plane of the film. In this case, the relative reduction of the bulk lattice parameter with respect to the substrate value is $a\rho$. Hence

$$a_s^* = a_s(1 - a\rho). \quad (4.1)$$

The variation of the lattice parameter of the ferroelectric from a_s to a_s^* takes place between the ferroelectric-substrate interface and the bulk, over a thin interfacial layer whose thickness is roughly the interdislocation distance ρ^{-1} . Using Eq. (4.1), the out-of-plane component of the strain gradient near the ferroelectric-substrate interface can be evaluated as

$$\frac{\partial \varepsilon_{11}}{\partial x_3} \cong \left(\frac{a_s - a}{a} - \frac{a_s^* - a}{a} \right) \bigg/ \rho^{-1} \approx \frac{\varepsilon_M^*}{a_s}, \quad (4.2)$$

where x_3 is the Cartesian coordinate normal to the plane of the film and $\varepsilon_M^* \equiv (a_s - a_s^*)/a$ is the amount of strain released by the misfit dislocations. The strain gradient is localized in a thin nearby-electrode layer of thickness $d \cong \rho^{-1} = a_s/\varepsilon_M^*$. Depending on the film thickness and on the conditions of strain relaxation in the film, ε_M^* varies between zero and the misfit strain $\varepsilon_M \equiv (a_s - a)/a$.

The flexoelectric effect can be described as an additional term $[\Delta F = g_{ijkl}^{(0)} P_i \partial \varepsilon_{jk} / \partial x_l]$ in the Landau free energy expansion.^{53–55} Being controlled by a fourth rank tensor, it is allowed in materials of any symmetry. To assess the poling efficiency of this effect, we estimate the value of the effective electric field, $E_i^{\text{eff}} = -\partial(\Delta F) / \partial P_i$, which would produce the same polarization as the strain gradient. Information on the value of the flexoelectric tensor components $g_{ijkl}^{(0)}$ in ferroelectrics are very limited; however, an order-of-magnitude estimate^{53–55} compatible with experimental data for perovskites⁵⁶ is $|g_{ijkl}^{(0)}| \cong e / (4\pi \varepsilon_0 a)$, where e stands for the electron charge. Using this estimate, we can write the value of the out-of-plane component of the effective electric field generated by the strain gradient as⁵⁷

$$\begin{aligned} E^{\text{eff}} &= g_{3311}^{(0)} \left(\frac{\partial \varepsilon_{xx}}{\partial z} + \frac{\partial \varepsilon_{yy}}{\partial z} \right) \\ &\cong \frac{2g_{3311}^{(0)}}{a} \varepsilon_M^* \cong \frac{2e}{4\pi \varepsilon_0 a^2} \varepsilon_M^* = 2E_{\text{at}} \varepsilon_M^*, \end{aligned} \quad (4.3)$$

where $E_{\text{at}} \approx 100$ MV/cm is the so-called typical atomic electric field. For epitaxial films, the misfit strain is typically about a 1%–5%. This gives an upper-limit estimate for the released misfit strain ε_M^* . Thus, according to Eq. (4.3), the strain gradient works as an electric field of some 20–500 kV/cm in a nearby-bottom electrode layer, which is a few tens of lattice constants thick.

It is clear that this effective electric field will impose some asymmetry on the switching behavior of the ferroelectric capacitor. Let us discuss these phenomena in terms of a simple model offered by Abe *et al.*,^{58,59} which is illustrated in Fig. 13. The model considers only two possible directions of polarization in the capacitor (“up” and “down”) and postulates that the strain gradient is large enough to block the polarization direction over a certain nearby-electrode layer.

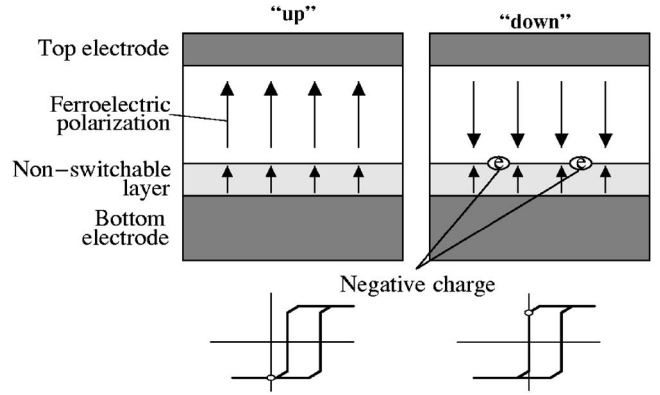


FIG. 13. The model devised in Refs. 58 and 59 to explain the voltage offset of ferroelectric loops in terms of the nearby-electrode poling effect of the strain gradient. In the convention adopted herein, the top electrode is grounded and the voltage is applied to the bottom electrode.

(Actually, flexoelectric coupling is not the only mechanism that can block switching in the passive layer; direct “microscopic” coupling between the polarization and the dislocation can also contribute to this blocking.¹³) The presence of a nonswitchable polar layer implies that one of the possible directions of polarization in the switchable part of the capacitor is preferable. In Fig. 13, this is the up direction. The state with reverse polarization is energetically less favorable, because it contains a head-to-head polarization configuration at the boundary between the switchable and non-switchable parts of the capacitor. The depolarization energy due to the bound charge at such boundary will make the down state of polarization energetically “costly.” If the depolarizing field is not compensated by free carriers, this state is metastable at best. However, if some free charge is accumulated at the interface between the switchable and nonswitchable parts, the down state can be stabilized. Thus, we arrive at a model similar to the one treated at the beginning of Sec. II E 1—cf. Eqs., (2.43)–(2.46); the difference is that now the passive layer is polar and affected by the effective electric field induced by the strain gradient. These features can be readily incorporated in the consideration by modifying Eqs. (2.44) and (2.45) as follows:

$$D_f - \sigma = \varepsilon_0 \kappa_d (E_d + E^{\text{eff}}) + P_M, \quad (4.4)$$

$$D_f - \sigma - P_M - \varepsilon_0 \kappa_d E^{\text{eff}} = \frac{\varepsilon_0 \kappa_d}{d} (V - hE_f), \quad (4.5)$$

where P_M is the spontaneous polarization in the strain-graded layer, $d \cong \rho^{-1} \cong a/\varepsilon_M^*$ is its thickness, and the rest of the notation has been introduced above in Sec. II E 1. Similar to the derivation of Eq. (2.46), we obtain for the voltage offset in the modified model:

$$V_{\text{off}} = -d \frac{P_M + \varepsilon_0 \kappa_d E^{\text{eff}} + \sigma}{\varepsilon_0 \kappa_d}. \quad (4.6)$$

This equation has the same physical meaning as Eq. (2.46): the voltage offset is controlled by the immobile charge at the ferroelectric-dielectric interface. While in the case of Eq. (2.46) such charge was simply the trapped free charge σ , now it is the sum of the bound charge associated with the

nonswitchable surface layer ($P_M + \varepsilon_0 \kappa_d E^{\text{eff}}$) and of the trapped free charge (σ). An expression for the voltage offset, similar to Eq. (4.6), was derived by Abe *et al.*,⁶⁰ but without taking into account the effective electric field E^{eff} produced by the misfit strain gradient.

For the model illustrated in Fig. 13, $P_M = P_s$ and it is constant during the switching. To evaluate the voltage offset, information on the compensating free charge at the interface are needed. If the up state is held long enough, the compensation charge σ may reach a value of $-\varepsilon_0 \kappa_d E^{\text{eff}}$, which corresponds to full screening of the field E_d in the strain-graded layer. According to Eq. (4.6), this corresponds to

$$V_{\text{off}} = -d \frac{P_s}{\varepsilon_0 \kappa_d}. \quad (4.7)$$

If this screening is not full, then $-\varepsilon_0 \kappa_d E^{\text{eff}} < \sigma < 0$. According to Eq. (4.6), this will alter the estimate (4.7). However, the relative variation of this estimate due to incomplete screening will not exceed $\varepsilon_0 \kappa_d E^{\text{eff}} / P_s$, which is expected to be much smaller than unity for the addressed case of temperatures not too close to the transition temperature. Then the estimate (4.7) should always be valid for the up state.

As to the down state, full screening of the bound charge requires the accumulation of a much larger amount of free charge at the interface between the switchable and nonswitchable regions: $\sigma = -2P_s - \varepsilon_0 \kappa_d E^{\text{eff}}$. This corresponds to a voltage offset of the opposite sign:

$$V_{\text{off}} = d \frac{P_s}{\varepsilon_0 \kappa_d}. \quad (4.8)$$

In contrast to the up state, the degree of screening (i.e., the variation of the charge in the range $-2P_s - \varepsilon_0 \kappa_d E^{\text{eff}} < \sigma < -\varepsilon_0 \kappa_d E^{\text{eff}}$) may essentially affect this estimate. So for the down state estimate (4.8) gives an upper limit for the possible positive offset. If for some reason the screening of this rather large bound charge is not complete, smaller positive offsets and even some negative offsets may occur.

The present model enables us to estimate the absolute value of a typical voltage offset induced by dislocation-assisted strain relaxation in epitaxial films. From (4.7) and (4.8), and taking into account that $d \cong a / \varepsilon_M^*$, we have

$$|V_{\text{off}}| \cong \frac{1}{\varepsilon_M^*} \frac{a P_s}{\varepsilon_0 \kappa_d}. \quad (4.9)$$

For realistic values of these parameters ($\varepsilon_M^* = 0.01$, $P_s = 0.25 \text{ C/m}^2$, $a = 0.4 \text{ nm}$, and $\kappa_d \cong \kappa_f = 150$, where $\kappa_d \cong \kappa_f$ follows from the *hard ferroelectric approximation*—cf. Sec. II E 1), we find $|V_{\text{off}}| \cong 8 \text{ V}$.

Notice that “surprisingly” the model predicts $|V_{\text{off}}|$ to be inversely proportional to the dislocation-assisted strain release ε_M^* . It is instructive to comment on this point. First, we recall that the thickness of the strain-graded layer (being inversely proportional to the misfit dislocation density) goes as $1/\varepsilon_M^*$, so that, for large amounts of strain released, the effect is extremely confined in space. Second, very high values of $|V_{\text{off}}|$ —which according to Eq. (4.9) imply very small values of ε_M^* —are beyond the range of applicability of this model. This is because, according to the model, the effective electric

field in the strain-graded layer, E^{eff} , is proportional to ε_M^{*2} and assumed to block the switching in this layer. It is clear that if ε_M^* is too small, the blocking effect of misfit dislocations may not be strong enough to prevent switching in the layer. In other words, for too small values of ε_M^* , the main assumption of the model—that the switching in the surface layer is blocked—ceases to hold.

B. Interface-stimulated nucleation

The nucleation of reverse domains in fields much smaller than the thermodynamic coercive field is a key problem in the theory of ferroelectric switching. This problem was addressed qualitatively by Merz,⁶¹ further quantitative considerations were offered by Landauer.⁶² These considerations were performed on the lines of the standard treatment of nucleation at a first-order phase transition. In the case of ferroelectric switching, the new feature is the need to take into account the energy of the depolarizing field in addition to the bulk and surface energy of the nucleus. Following the usual logic of nucleation problems, the energy U_c of the critical nucleus (i.e., the nucleus having the minimum energy of all the nuclei which are unstable with respect to further expansion) was calculated and the nucleation rate was evaluated as proportional to the Gibbs factor $\exp(-U_c/k_B T)$. In its original form, the Landauer theory encounters a serious problem—namely, the value of the activation barrier U_c was found to be unrealistically large ($U_c = 10^8 k_B T$ for BaTiO₃ at room temperature and under an applied field $E = 0.5 \text{ kV/cm}$, cf. Ref. 62). Even at the very high applied fields routinely used in ferroelectric thin film capacitors, this energy remains too high to provide realistic nucleation rates [$U_c = 10^3 k_B T$ for PZT films at room temperature and $E = 100 \text{ kV/cm}$, giving a Gibbs factor of $\exp(-U_c/k_B T) \cong 10^{-430}$, cf., e.g., Ref. 63]. All these estimates have been obtained for the case of nucleation in an ideal insulating crystal, i.e., for nucleation that is not assisted by the presence of defects or free carriers in the material. Since the switching from single-domain states always takes place experimentally at fields essentially smaller than the thermodynamic coercive field, it was commonly assumed that, in real crystals, the nucleation of new domains is always defect assisted. Revision of the Landauer theory on the lines of this scenario has been recently undertaken by Molotskii *et al.*⁶⁴ and Gerra *et al.*⁶⁵ Molotskii *et al.* have shown that the simultaneous formation of a Landauer nucleus and of an electron droplet may be energetically favorable; however, the results of their work cannot be reliably translated into an estimate for the nucleation rate. Gerra *et al.* have generalized the Landauer model by incorporating the energy of the ferroelectric-electrode interface, which is dependent upon the sign of polarization at the interface. The latter model was able to provide a realistic description of reverse domain nucleation. We will now present the Landauer model and its modified version.

Landauer⁶² considered the nucleus of a reverse domain, having the form of half a prolate spheroid (of radius r and length l) and terminating on one electrode (Fig. 14). Its en-

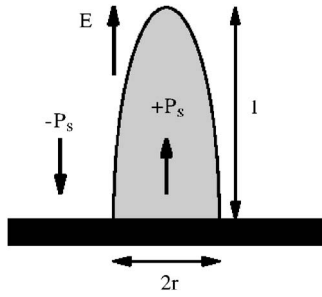


FIG. 14. Nucleus of a reverse domain in a “down-polarized” ferroelectric material which has its polar axis in the vertical direction and normal to the electrode. An external field E in the “up” direction is applied to the system.

ergy (i.e., the variation of the thermodynamic potential of the capacitor kept under a fixed voltage, due to the formation of the nucleus) can be written as⁶⁶

$$U = -ar^2l + brl + c\frac{r^4}{l}, \quad (4.10)$$

$$a \equiv \frac{4}{3}\pi EP_s, \quad b \equiv \frac{\pi^2}{2}\sigma_w, \quad (4.11)$$

$$c \equiv \frac{16\pi^2 P_s^2}{3\epsilon_0 \kappa_a} \left[\ln \left(\frac{2l}{r} \sqrt{\frac{\kappa_a}{\kappa_c}} \right) - 1 \right].$$

Here, σ_w , κ_c , and κ_a are the surface energy of a 180° wall, and the relative lattice dielectric constants in the direction of the spontaneous polarization and perpendicular to it, respectively. The parameters r and l of the critical nucleus (r_L and l_L) and its energy (U_L) were routinely determined from minimization of U . The condition $\partial U / \partial l = 0$ yields a global minimum of U with respect to l at

$$l = \sqrt{\frac{cr^3}{b-ar}}. \quad (4.12)$$

This result, together with the condition $\partial U / \partial r = 0$, gives

$$r_L = \frac{5b}{6a}, \quad l_L = r_L \sqrt{\frac{5c}{a}}, \quad U_L = 0.4ar_L^2 l_L. \quad (4.13)$$

Using these expressions, we arrive at the previous estimates for the energy of the critical nucleus, which are exceeding the thermal energy by several orders of magnitude. For instance, the estimate $\exp(-U_c/k_B T) \approx 10^{-430}$ for a PZT film at $E = 100$ kV/cm can be obtained by setting $P_s = 30$ $\mu\text{C}/\text{cm}^2$, $\sigma_w = 0.01$ J/m², and $\kappa_a = \kappa_c = 200$.

The activation energy of nucleation can be essentially reduced by assuming that the surface energy of the ferroelectric-electrode interface depends essentially on the sign of the polarization component normal to the electrode. This asymmetry can be due to electronic or mechanical properties of the interface and/or the presence of impurities or dislocations, and from a theoretical point of view it follows from the fact that, in general, the surface breaks the inversion symmetry of the crystal. Since the free energy of a ferroelectric is a function of the vector of polarization, which determines the symmetry of the crystal, then the free energy is affected by the presence of the surface through the coupling

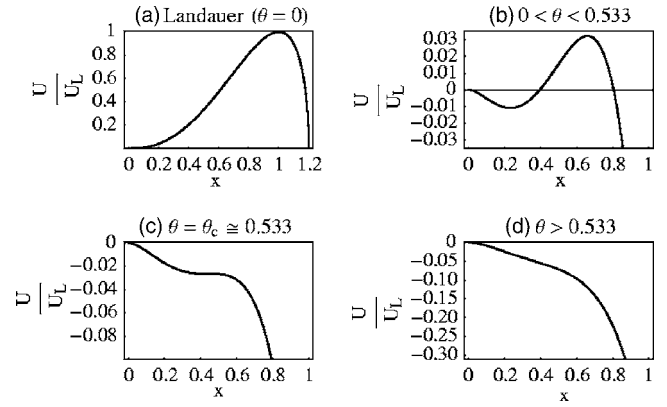


FIG. 15. The effect of parameter ϑ on the domain energy (normalized to the Landauer activation energy U_L). The nucleation barrier and critical size (i.e., the point of maximum x_{\max}) both decrease with increasing ϑ values.

of polarization with the surface itself. Because of the inversion-symmetry breaking, the free energy is in general dependent on the sign of this coupling, that is, on the sign of polarization at the surface. We can therefore expand the ferroelectric-electrode coupling energy per unit area, γ , in terms of the surface polarization, including both even and odd terms.⁶⁷ In the simplest case, we can write $\gamma = \zeta P_s$. This linear term, ζP_s , is analogous to the free energy per unit volume term due to the applied field, $E_{\text{ext}} P_s$, and accordingly, the coefficient ζ can be seen as the *surface analog* of the field conjugate to the order parameter.

One incorporates this phenomenon into the Landauer model by adding a new term to the energy given by Eq. (4.10):

$$U_{\text{int}} = \gamma \pi r^2. \quad (4.14)$$

With this term taken into account, the energy of the nucleus as a function of its normalized radius ($x \equiv r/r_L$) has the form⁶⁵

$$\frac{U(x)}{U_L} = \sqrt{6}x^2 \left[\sqrt{x \left(1 - \frac{5}{6}x \right)} - \sqrt{\frac{5}{6}}\vartheta \right], \quad (4.15)$$

$$\vartheta \equiv \frac{\pi\gamma}{2b} \sqrt{\frac{a}{c}}.$$

Figure 15 shows a plot of $U(x)$ for different values of the parameter ϑ . In the original Landauer model, where $\vartheta = 0$, we had a local minimum at $r = l = 0$ and a saddle point at $r = r_L$ [Fig. 15(a)]. For nonzero values of ϑ , the point $x = 0$ becomes unstable, the local minimum U_{\min} is shifted to the right, and the local maximum U_{\max} to the left, while the activation energy, $\Delta U = U_{\max} - U_{\min}$, is decreased [Fig. 15(b)]. Here, $U_{\min} = U(x_{\min})$ and $U_{\max} = U(x_{\max})$, where x_{\min} and x_{\max} are the positive roots of the following equation:

$$\frac{5\sqrt{5x(1-x)}}{4\sqrt{6-5x}} = \vartheta. \quad (4.16)$$

When the parameter ϑ exceeds its critical value, $\vartheta_c \approx 0.553$, Eq. (4.16) has no positive roots and the activation barrier disappears [Figs. 15(c) and 15(d)]. Unlike the classical Landauer model, we arrive at the situation where, for applied

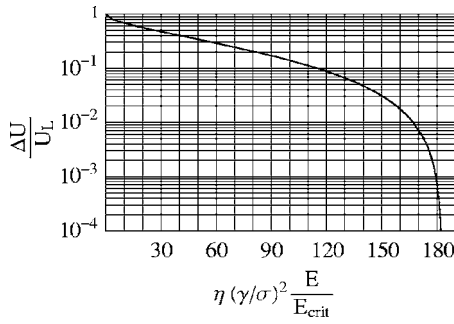


FIG. 16. Nucleation barrier ΔU (normalized to the Landauer value U_L) as a function of the anisotropy factor η , the external field E , and the ratio γ/σ_w .

fields corresponding to the condition $\vartheta > \vartheta_c$, the nucleation barrier is completely suppressed.

It is instructive to express ϑ in terms of the anisotropy factor, $\eta = \kappa_a/\kappa_c$, and of the thermodynamic coercive field, $E_{\text{crit}} = P_s/(3\sqrt{3}\epsilon_0\kappa_c)$:^{68,69}

$$\vartheta = k \frac{\gamma}{\sigma_w} \sqrt{\eta \frac{E}{E_{\text{crit}}}}, \quad (4.17)$$

with $k \approx 0.04$.

Figure 16 is a plot of the activation energy $\Delta U = U_{\text{max}} - U_{\text{min}}$ as a function of the physical quantities appearing in (4.17). It is evident that as well as by the external electric field, nucleation is favored by high values of the interface to domain wall energy density ratio, γ/σ_w , and of the anisotropy factor η . The latter, less evident effect is related to a reduction of the electrostatic energy, which is inversely proportional to the transverse permittivity κ_a —cf. Eq. (4.11). From the condition $\vartheta > \vartheta_c$ and Eq. (4.17), one obtains the applied field needed for the total suppression of the nucleation barrier, which we will call *zero-temperature* critical field $E_c^{T=0}$:

$$\frac{E_c^{T=0}}{E_{\text{crit}}} \approx \frac{183}{\eta} \left(\frac{\sigma_w}{\gamma} \right)^2. \quad (4.18)$$

In Fig. 16, we note that the nucleation barrier drops to zero abruptly as the applied field approaches $E_c^{T=0}$. For fields less than 70% of the critical value, $\Delta U \geq 0.1 U_L$, implying, for typical values of the relevant parameters, unrealistically low nucleation rates. This means that, in the modified model, the finite-temperature critical field is within 30% of $E_c^{T=0}$. Moreover, if the nucleation is the limiting factor of switching, then the coercive field measured in hysteresis loops is close to this finite-temperature critical field and does not diverge when the temperature is decreased.

Two more features following from the above analysis are worth mentioning. First, nucleation has been found to be favored by a high value of the anisotropy factor η . This implies that the switching can be facilitated in perovskite-type ferroelectrics near morphotropic phase boundaries, where this factor is anomalously high. This prediction may be relevant to the coercive field reduction in $\text{PbZr}_x\text{Ti}_{1-x}\text{O}_3$ at the tetragonal side of the morphotropic phase boundary.⁷⁰ Second, the model predicts the possibility of an exponentially wide spectrum of waiting times for nucleation. It is clear from Fig. 16 that, in the steep part of the curve (corre-

sponding to a realistic thermoactivation regime), small variations of the system parameters readily lead to orders-of-magnitude variations of the activation barrier, on which the waiting time is exponentially dependent. This result is important in the context of the data on the switching kinetics in ferroelectric thin films, which have been interpreted in terms of this kind of spectrum.⁷¹ For the moment, due to the absence of experimental data and results of first-principle calculations for the energy of the ferroelectric-electrode interface, it is difficult to estimate the strength of the effects discussed above. However, according to Gerra *et al.*,⁶⁵ rough order-of-magnitude estimates suggest that the ferroelectric-electrode interaction can significantly facilitate the switching. Using the Landau theory result for the domain wall energy $\sigma_w = t_w P_s E_{\text{crit}} \sqrt{3}/2$ (where t_w is the wall thickness), and the so-called “atomic” estimate $\zeta \cong E_{\text{at}} l_{\text{at}}$ for the effective surface field (where $E_{\text{at}} \cong 100$ MV/cm is a typical atomic electric field and l_{at} is the lattice constant), we get $\sigma_w/\gamma = \sigma_w/(P_s \zeta) \cong (E_{\text{crit}}/E_{\text{at}})(t_w/l_{\text{at}})$. Bearing in mind parameters of perovskite ferroelectrics such as BaTiO_3 , we find that the ratio σ_w/γ may be as small as 10^{-2} . Thus, according to Eq. (4.18), the model can yield a coercive field two orders of magnitude smaller than E_{crit} . Taking room temperature parameters of BaTiO_3 ($P_s = 26 \mu\text{C}/\text{cm}^2$, $\kappa_a = 2000$, $\kappa_c = 120$, and $\sigma_w \cong 7 \times 10^{-7} \text{ J}/\text{cm}^2$) and $\sigma_w/\gamma = 0.02$, one obtains $E_c^{T=0} \cong 2 \text{ kV}/\text{cm}$. This estimate shows that the model may provide reduction of the coercive field down to typical values for BaTiO_3 single crystals (about 1 kV/cm).

The above considerations were made for a situation where the surface field ζ is homogeneous, which may not be a realistic assumption. While small variations in the magnitude of ζ do not alter the qualitative features of the model, fluctuations in the sign of ζ might have important consequences. If the typical radius of the regions where ζ is homogeneous, r_0 , is greater than the Landauer critical radius r_L , then nucleation will not be affected by variations of ζ . On the other hand, if $r_0 < r_L$, fluctuations in the sign of ζ will result in opposite contributions to the energy—i.e., different parts of the interface support different orientations of the polarization. The latter situation requires a more involved analysis. The case of small-scale inhomogeneities of ζ (i.e., $r_0 \ll r_L$) has been treated by Gerra *et al.*⁶⁵ on the lines of the Imry-Ma statistical approach.⁷² Results similar to those presented above have been obtained, though with higher values of the zero-temperature critical field $E_c^{T=0}$.

C. Poling effect of the interface and dielectric permittivity

In Sec. IV B, we have seen that the coupling between the ferroelectric and the electrodes can aid the nucleation process substantially, through the *surface field* ζ . We will now see that this coupling has other important consequences.

In Ref. 73, Bratkovsky and Levanyuk considered the effect of ζ on the dielectric constant and the phase transition, showing that the latter is considerably smeared out by the coupling with polarization.⁷⁴ To prove this, the authors included the ferroelectric-electrode coupling energy density, γ , into the Landau-Devonshire free energy expression given by

Kretschmer and Binder¹⁸ (i.e., taking into account the depolarizing field, cf. Sec. II C). The inclusion of this coupling term modifies the boundary conditions (2.29), which for the general case of asymmetric ferroelectric-electrode coupling become^{73,75}

$$\lambda^{-1}P_1 - \left. \frac{\partial P}{\partial x} \right|_{x=0} = \frac{\zeta_1}{\delta}, \quad \lambda^{-1}P_2 + \left. \frac{\partial P}{\partial x} \right|_{x=h} = \frac{\zeta_2}{\delta}, \quad (4.19)$$

where $P_i = P(x_i)$ are the values of polarization at the two surfaces ($x_1=0$ and $x_2=h$), λ is the extrapolation length introduced in Sec. II C, and δ is the coefficient of the gradient term of the free energy—cf. Eq. (2.19). We see from Eq. (4.19) that the effect of the ferroelectric-electrode interface is to “pole” the film at the surface. The sign of poling depends on the sign of ζ_i .

Let us discuss, for simplicity, the case of a second order phase transition. The equation of state of the system can be found by minimizing the free energy functional, cf. Eq. (2.26):

$$\alpha P + \beta P^3 - \delta \frac{\partial^2 P}{\partial x^2} = E_{\text{ext}} - \frac{1}{\epsilon_0 \kappa_b} (P - \bar{P}), \quad (4.20)$$

where E_{ext} is the applied electric field, and \bar{P} the average polarization in the film. The local polarization profile $P(x)$ can be found by solving the differential equation (4.20) with boundary conditions (4.19). Since the boundary conditions are, in general, asymmetric, then the solution of (4.20) will not be a symmetric function—unlike Eq. (2.27). However, the polarization will reach its bulk value exponentially fast and over the same distance $\xi_1 = \sqrt{\delta \epsilon_0 \kappa_b}$ as before.

One should bear in mind that, as pointed out already in Sec. II C, ξ_1 is typically less than the lattice parameter of the ferroelectric crystal, and therefore the problem is outside the range of applicability of a continuous theory such as Landau-Devonshire's. Nevertheless, it is instructive to use the results of the theory as a semiempirical model for the effect of surface poling on permittivity.

Assuming that $\xi_1 \ll \lambda$, Bratkovsky and Levanyuk showed that the dielectric constant of the ferroelectric film is⁷³

$$\kappa_{\text{eff}} = \frac{1}{\epsilon_0} \frac{1}{\tilde{\alpha} + 3\beta \bar{P}^2}, \quad (4.21)$$

where $\tilde{\alpha}$ is the renormalized linear coefficient, Eq. (2.31) with $d/\kappa_d = 2\xi_1/\kappa_b$. Using the result of Bratkovsky and Levanyuk,⁷³ not too close to the phase transition, the average polarization in the film can be roughly estimated as

$$\bar{P} \approx \frac{1}{\tilde{\alpha}} \left(\frac{\zeta_1 + \zeta_2}{h} \right), \quad (4.22)$$

whereby the effective inverse permittivity of the film has the form

$$\kappa_{\text{eff}}^{-1} \approx \tilde{\alpha} \epsilon_0 + \frac{3\beta \epsilon_0}{\tilde{\alpha}^2} \left(\frac{\zeta_1 + \zeta_2}{h} \right)^2, \quad (4.23)$$

which, in the case of symmetric ferroelectric-electrode coupling ($\zeta_1 = -\zeta_2$), reduces to the result of Kretschmer and Binder, Eqs. (2.28) and (2.30) in the approximation $\xi_1 \ll \lambda$.

Note that the term $3\beta \bar{P}^2$ in the denominator of Eq. (4.21) is temperature dependent, through the temperature dependence of $\tilde{\alpha}$ —cf. Eqs. (4.22) and (2.31). If it were not so, its effect would be to further renormalize the Curie-Weiss temperature of the phase transition, which is exactly the effect of the presence of passive layers. But through its temperature dependence, surface poling has the effect of smearing out the phase transition, i.e., of drastically flattening the peak of the dielectric constant as a function of temperature. Using the estimate $\zeta \sim E_{\text{at}} l_{\text{at}}$, we may expect to observe smearing by values as high as ~ 100 K in, e.g., 100-nm-thick films of $\text{Ba}(\text{Sr}, \text{Ti})\text{O}_3$.⁷³

It is worth mentioning that this scenario for the smearing of the ferroelectric phase transition in thin films may be experimentally verified. The point is that the poling effect of the interface should manifest itself not only by smearing the phase transition but also by inducing a piezoelectric response above the transition temperature. A clear correlation between the size of this effect and the degree of smearing is expected. Experimental identification of this correlation would provide strong support for the scenario in question.

V. INTERNAL BIAS FIELD AND IMPRINT: THEORY VERSUS EXPERIMENTAL OBSERVATIONS

A number of experimental techniques have been used for observation and characterization of internal bias field effects in ferroelectric thin films. The method mostly used for the characterization of internal field effects is to monitor the coercive voltages of electric-field-driven hysteresis loops of different parameters of the film, such as polarization,^{76,77} differential capacitance,⁵⁸ or the longitudinal piezoelectric coefficient “ d_{33} .”^{78,79} In this method, the voltage offset, $V_{\text{off-cr}}$, is calculated as the half-sum of the measured coercive voltages (taken with their sign). This method is quite illustrative; however, it is not optimal for qualitative characterization of the phenomenon. Two of its main drawbacks have been discussed in Sec. II E 1. First, relating the half-sum of the coercive voltages of a polarization loop with the real voltage offset, V_{off} , may pose a serious problem, due to the difference in saturation at the tips of the loop introduced by the internal bias. Second, for P - E loops, the polarization offset is conventionally set to zero, while in the presence of internal bias the switching driven by a “symmetric” ac field is intrinsically “asymmetric.” This artificial elimination of the polarization offset of the loop can bring about an additional, spurious voltage offset, which can be substantial. Although we have discussed these problems in detail only for the voltage offset mechanism related to trapped charge, it is clear that for any voltage offset mechanism there may be some difference between the real voltage offset and that calculated from the coercive voltages of the P - E loop. For the case of d_{33} - E loops, the situation may be even worse. If the polarization in a part of the film is frozen in one direction, whereas in the rest of the film the switching is symmetric but with a tilted loop, the resulting d_{33} - E loop will exhibit a spurious voltage offset, associated with a vertical shift of the loop controlled by the frozen polarization. The latter may not be related to the presence of internal bias. From the point of view of

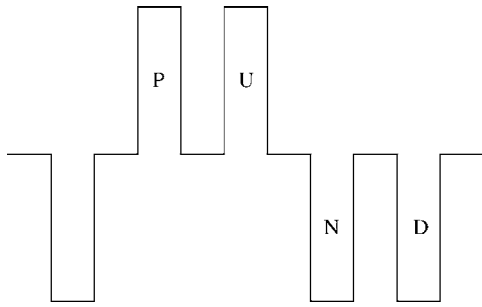


FIG. 17. The *PUND* method used for the characterization of internal field effects in ferroelectric capacitor systems. The capacitor is subjected to a sequence of positive (*P* and *U*) and negative (*N* and *D*) voltage pulses, and for each pulse $i=P, U, N, D$ the switching charge Q_i is measured. The difference between Q_N and Q_P gives information about the sign of the internal bias field.

memory applications (for which control of the imprint is of primary importance), the hysteresis-loop-based method discussed here is not really informative, since, in these applications, it is the fast pulse technique that is used, rather than the relatively slow hysteresis technique.

The method of characterization of the internal field effects, which is the most common in memory applications of ferroelectric thin films, is the so-called *PUND* test proposed by Traynor *et al.*⁸⁰ In this test, the tested capacitor is subjected to the sequence of voltage pulses shown in Fig. 17, and the charges Q_P , Q_U , Q_N , and Q_D (switched by pulses *P*, *U*, *N*, and *D*, respectively) are collected. In the case of a capacitor not affected by an internal bias field, $Q_P=Q_N > Q_U=Q_D$. If it is affected, the information on the internal bias field are provided by the difference between Q_P and Q_N . If the internal bias field is positive, the switching from the positively poled state to the negatively poled one will be less efficient than in the case of the opposite sense of switching, resulting in $Q_P < Q_N$ and vice versa. The advantage of this method is that it evaluates the impact of the internal bias field on the charges Q_P and Q_N used for reading the information bit stored in the capacitor. On the other hand, the value of the voltage offset is not directly given by this technique.

There are also techniques that directly provide the value of the voltage offset for the pulse switching regime. The basic idea of these approaches is to compare voltages applied to the capacitor that produce the same switching effects in the case where the internal bias field is directed along the applied field, against it, or when it is absent. This approach has been used by Abe *et al.*⁸¹ to evaluate the built-in internal bias in BaTiO₃ thin films, by comparing the voltage giving the same value of the maximum switching current, for each sense of switching. Figure 18(a) exemplifies this method. In this figure, the maximum switching current is plotted as a function of the amplitude of the applied positive and negative voltage pulses. The voltage shift between the curves corresponding to two signs of the applied field is about 0.9 V, which can be interpreted as the presence of a voltage offset $V_{\text{off}}=0.45$ V. For comparison, a *P-E* loop taken from the same film is shown in Fig. 18(b). The coercive voltages of this loop give a value of the voltage offset close to that

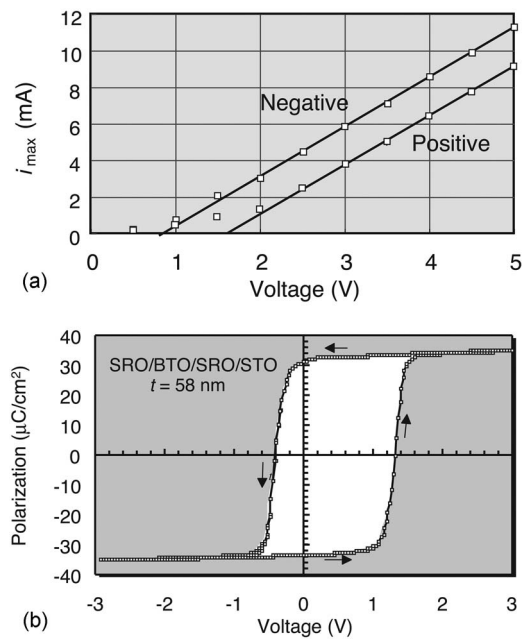


FIG. 18. (a) The method used by Abe *et al.* (Ref. 81) to evaluate the built-in internal bias in BaTiO₃ thin films by comparing the value of the maximum switching current for each sense of switching. (b) The *P-E* loop for the same film. Good agreement is observed between the voltage offsets determined from the i_{max} measurements and from the *P-E* loop. After Ref. 81.

determined from the data on switching currents. This may be expected, since the loop is saturated and quite rectangular.

A similar method based on this idea has been used by Tagantsev *et al.*³⁵ for imprint characterization. In this method, the charge obtained by switching against the internal bias field of the imprinted capacitor is compared to the corresponding switching charge of the nonimprinted capacitor. Then, the difference between these charges, ΔP , is converted into a voltage offset by using the voltage dependence of the switching charge for the nonimprinted capacitor. Figure 19 illustrates the application of this method to the evaluation of the exposition time and temperature dependence of imprint in (Pb,La)(Zr,Ti)O₃ (PLZT) film capacitors. Figure 19(a) shows the exposition-time dependence of ΔP , acquired at different exposition temperatures with voltage pulses of 1.8 V. Figure 19(b) shows the voltage dependence of the switching charge used for data conversion. Because of the linear character of this curve below 2 V, for 1.8 V pulses, the conversion relation can be written as

$$V_{\text{off}} = A \Delta P, \quad (5.1)$$

with $A=0.041$ V cm²/μC. Finally, Fig. 19(c) shows the determined exposition time and temperature dependence of V_{off} .

A feature of the voltage offset often discussed in the literature is its increasing dependence on the film thickness.^{37,58,77} Data illustrating this trend for built-in internal bias in BaTiO₃ films and for photoinduced imprint on PZT films are presented in Fig. 20. The interpretation of this trend still remains unclear. In all the aforementioned papers, the internal bias effect is attributed either to nearby-electrode charge trapping^{37,77} or to the nearby-electrode strain gradient.⁵⁸ On the other hand, as shown in Sec. IV A, the

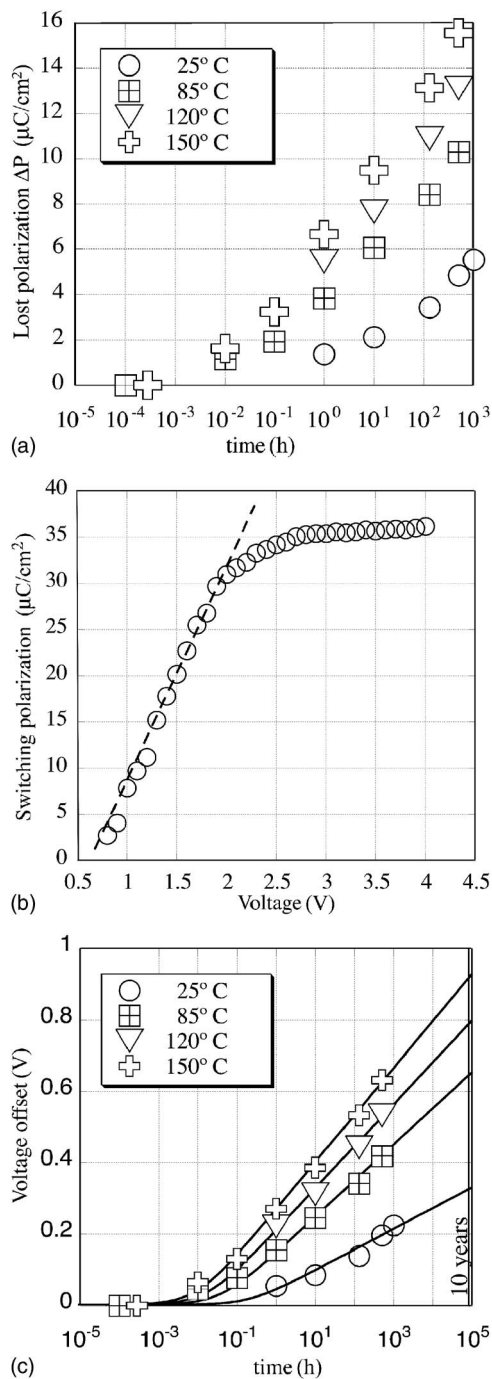


FIG. 19. Imprint in PLZT film capacitors: (a) difference between the switching charge of the imprinted and the nonimprinted capacitor, ΔP , as a function of exposition time for different exposition temperatures; (b) switching charge as a function of applied voltage; and (c) calculated voltage offset as a function of exposition time and exposition temperature. After Ref. 35.

strain-gradient mechanism implies no explicit thickness dependence of the voltage offset, whereas the charge trapping mechanism predicts a certain thickness dependence of the voltage offset only in a rather special case,⁸² when $d/\kappa_d \gg h/\kappa_f$ —cf. Eqs. (2.54), (2.66), (2.70), and (2.74). So there seems to be a problem with the interpretation of this phenomenon in terms of the models used by these authors. This suggests that other voltage offset mechanisms [related to the depletion effect, Eq. (3.7), or to reorientable defects—cf. Ref. 83], providing a linear thickness dependence of V_{off} ,

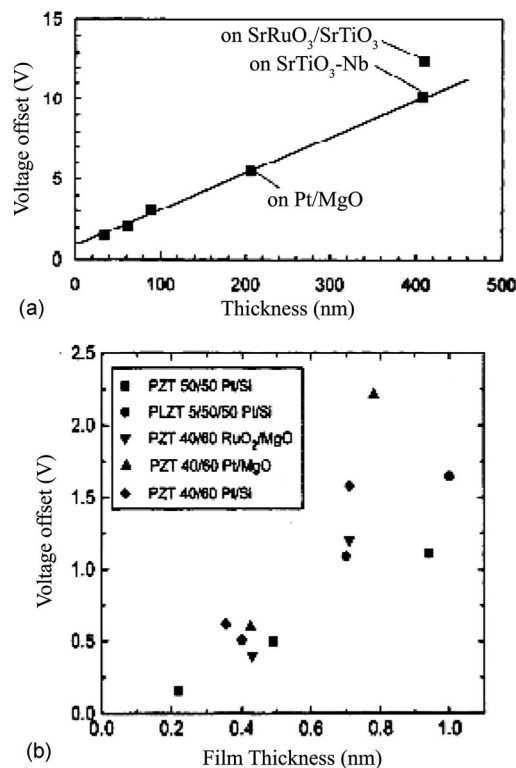


FIG. 20. Thickness dependence of the voltage offset measured in (a) BaTiO₃ films with built-in internal bias (after Ref. 58) and (b) PZT films with photoinduced imprint (after Ref. 77).

may apply to these systems. Alternatively, an implicit thickness dependence of the voltage offset—e.g., through the thickness dependence of the remanent polarization—may give an explanation in terms of the mechanisms proposed by these authors.

Experimental investigations of the built-in voltage offset in Pt/PZT/Pt thin film capacitors clearly reveal a composition dependence of this phenomenon; specifically, it was documented that the higher the titanium concentration, the stronger the built-in voltage offset.^{78,84,85} This effect is illustrated in Fig. 21(a), where the built-in field of sputtered 300-nm-thick PZT films is plotted as a function of Zr content. This effect was equally reported for sputtered and sol-gel deposited films. The original voltage offset was found to be removable by annealing at 350–450 °C.^{78,84,86} This is illustrated in Fig. 21(b). Kholkin *et al.*⁷⁸ have interpreted the annealing-assisted removal of the voltage offset in terms of the depletion-assisted scenario. In as-fabricated PZT capacitors, the Pt top electrode is deposited at room temperature, whereas the bottom electrode/PZT interface is exposed to 600–650 °C for some 15–30 min. This creates an asymmetry in the depletion of electrons from deep trapping states in PZT. No depletion is expected at the top electrode in the as-fabricated capacitor, because room temperature is presumably too low to establish electrochemical equilibrium near this electrode. In terms of the theoretical treatment given in Sec. III A 2, this is equivalent to a difference in the built-in surface potentials in Eq. (3.5) on page 32, which can lead to a built-in voltage offset. After the annealing, electrochemical equilibrium is expected to be established at the top electrode,

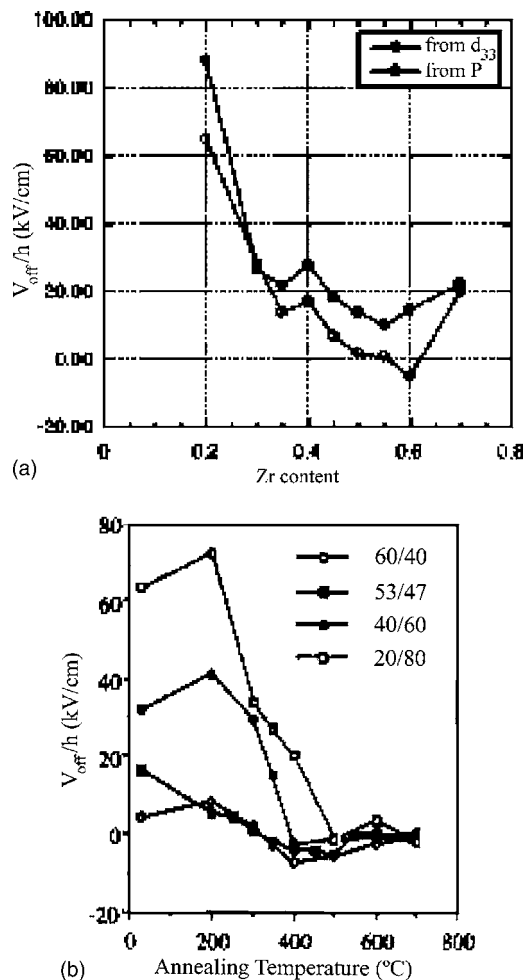


FIG. 21. (a) The effect of Zr/Ti ratio on the voltage offset evaluated from the piezoelectric and polarization loop measurements (after Ref. 85), and (b) the effect of annealing at 350–450 °C on the voltage offset for different values of the Zr/Ti ratio (after Ref. 84).

leading to equilibration of the built-in surface potentials and suppression of the built-in voltage offset. The thickness dependence of the voltage offset reported by Kholkin *et al.*⁷⁸ is qualitatively compatible with the theoretical predictions of Eqs. (3.7) and (3.8).

At this point, we would like to draw the reader's attention to the difference between built-in internal field and built-in polarization. There are many ways of determining the former (as discussed above), while the latter can be practically determined only from pyroelectric⁷⁶ or piezoelectric measurements—it is typically evaluated from the d_{33} offset of a piezoelectric hysteresis loop.⁷⁸ In principle, the behavior of the built-in internal field and of the built-in polarization may be very different, since the built-in polarization gives information both on the asymmetry of switching in the active part of the film and on the net polarization of the nonswitchable (“frozen”) part of the film, whereas the built-in internal field gives information only on the former. A correlation between these parameters (e.g., as a function of film composition) and their uncorrelated behavior have both been reported.^{78,85} Figure 21(a) illustrates the situation where such correlation is observed.

The built-in internal field has been reported to be influ-

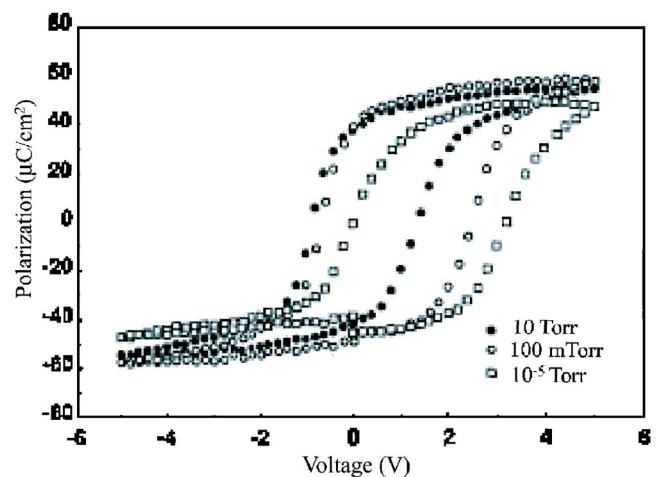


FIG. 22. Effect on the built-in internal field of the oxygen pressure at which a PZT capacitor with oxide electrodes was maintained during cooling. The voltage offset of the P - E loop increases with decreasing oxygen pressure. After Ref. 87.

enced by the value of the oxygen pressure maintained during cooling of the films from the crystallization temperature down to room temperature.^{87,88} This effect is illustrated in Fig. 22, where the voltage shift of the P - E loop as a function of oxygen pressure is shown for a PZT capacitor with oxide electrodes. The authors attributed this effect to the coupling of the ferroelectric polarization with oxygen vacancies (the concentration of the latter is assumed to be correlated with the oxygen pressure maintained during cooling). Experimental data that can also indicate the role of oxygen vacancies in the formation of built-in field in PZT thin films have been reported on imprint in donor-doped (Nb, Ta, and W substitutions for Ti) films.⁸⁹ In this work, doping was found to reduce the thermally induced imprint. This reduction was related to that of the oxygen vacancy concentration accompanying the doping (similar to the case of bulk PZT ceramics). Remarkably, in the same material, the authors found that UV-light illumination-assisted (“optical”) imprint was virtually insensitive to this kind of doping. This suggests that electronic defects rather than oxygen vacancies are active in optical imprint. This observation together with other observations from the literature suggest that more than one imprint mechanism can be active in one material.

The dependence of the imprint-induced voltage offset on the exposition time has been found to be logarithmically slow. For an empirical fit of this dependence, different single functions and combination of functions have been used—for instance, a single logarithm function,⁸⁰ two logarithm functions with different parameters at small and large times,⁹⁰ and a stretched exponential function.⁷⁷ The experimental data on the exposition time and temperature dependence of the imprint-induced voltage offset in PZT films have been analyzed in terms of the nearby-electrode trapping model discussed earlier in Sec. II E 2. Grossman *et al.*³⁷ performed numerical simulations in terms of this model, assuming Poole-Frenkel emission (with activation barriers of 0.35 eV) to be the conduction mechanism in the nearby-electrode passive layer. The imprint data by Tagantsev *et al.*,³⁵ already shown in Fig. 19(c), have been fitted in terms of the analyti-

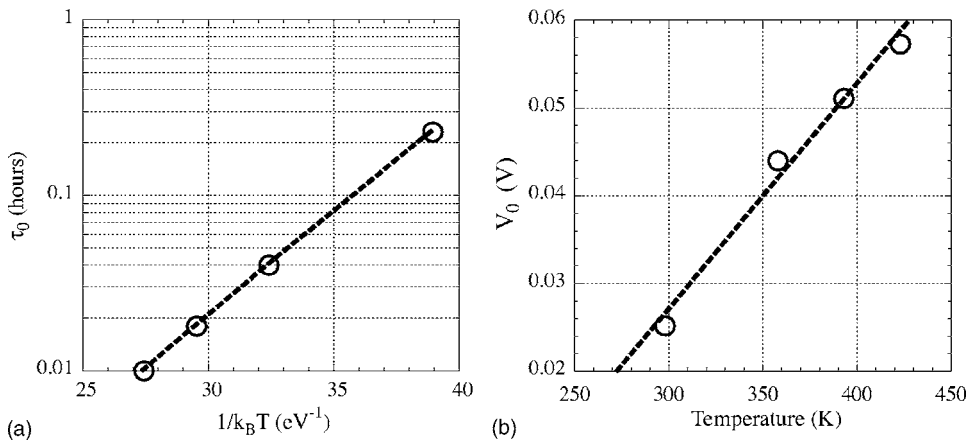


FIG. 23. Temperature dependence of the parameters V_0 and τ_0 appearing in the analytical theory for imprint due to nearby-electrode trapping—cf. Eqs. (2.66), (2.70), and (2.71). These parameters have been determined from the fit of the time dependence of the voltage offset, shown in Fig. 19(c).

cal theory for nearby-electrode trapping—Eqs. (2.66), (2.70), and (2.71)—for the case of thermoionic or Poole-Frenkel emission. A fit of the time dependence of the voltage offset is shown in Fig. 19(c). The parameters of the theory, V_0 and τ_0 , determined from this fit, are plotted as a function of temperature in Fig. 23. It is seen that the theory provides a good description of the time dependence of imprint observed in this experiment. The theoretical predictions for the temperature dependence of V_0 and τ_0 are also in qualitative agreement with the trends observed experimentally: the experimentally determined value of τ_0 is an exponential function of temperature (with an activation energy of 0.27 eV), whereas V_0 is a linear function of temperature. However, it is clear that the theory is too rough to give a thorough quantitative description of the experimental observations. For example, the theory predicts no offset in the linear temperature dependence of V_0 , when a substantial negative offset is observed experimentally [Fig. 23(b)].

VI. CONCLUSIONS

We have presented a review of current theoretical approaches to the description of interface-induced phenomena affecting the polarization response of ferroelectric thin films. These approaches enable a rationalization of several features documented in this context. The following general remarks summarize the principal conclusions of the paper and underline the main achievements needed for further development of the subject.

“Passive layer” effects manifest themselves clearly in the polarization response of thin films. An important task is to identify which of these effects (i.e., surface polarization blocking, Thomas-Fermi screening, or depletion) is foremost in real systems. The most popular of these three scenarios, the surface polarization blocking mechanism, seems to be the less probable candidate. This is due to the fact that, in any situation of interest, the continuous theory of Kretschmer and Binder deals with a polarization variation on a scale which is smaller than the lattice constant. This makes the theory non-self-consistent, and its quantitative predictions are therefore not reliable. Furthermore, when the background dielectric permittivity is taken into account, the theory predicts a negligible effect on the total permittivity. As to the second scenario, related to the finite thickness of the charge layer in the

electrodes (Thomas-Fermi screening), the effect appears to be strong enough to affect the polarization response of ferroelectric thin films in an appreciable way. Finally, the impact of depletion space charge on the polarization response of ferroelectric thin films can also be appreciable. However, to demonstrate its relevance to size effects observed in real systems, a more detailed, complex analysis of the defect chemistry and polarization response is required.

The problem of internal bias and imprint in ferroelectric thin films has received much attention by both the experimental and the theoretical community. Despite the clear progress achieved in sorting out these phenomena through realistic theoretical models, one issue is still ill understood—namely, the thickness dependence of the internal bias field, both in the case of built-in fields and of imprint.

A recent phenomenological analysis of the poling effect of the ferroelectric-electrode interface has shown that this effect may be of key importance to the polarization response of ferroelectric thin films, showing an equally strong impact on both switching and small signal response. The question of true relevance of this effect to the properties of ferroelectric thin films requires more experimental and theoretical efforts. From the theoretical point of view, it is crucial to obtain reliable estimates for the ferroelectric-electrode coupling as a function of polarization direction.

ACKNOWLEDGMENTS

This project was supported by the Swiss National Science Foundation.

¹A. K. Tagantsev, M. Landivar, E. Colla, and N. Setter, J. Appl. Phys. **78**, 2623 (1995).

²C. J. Brennan, Ferroelectrics **132**, 245 (1992).

³S. L. Miller, R. D. Nasby, J. R. Schwank, M. S. Rogers, and P. V. Dressendorfer, J. Appl. Phys. **58**, 6463 (1990).

⁴The application of this formula to the comparison of the slope of loops for the sandwich and the ferroelectric taken at the same amplitude of the driving field E_m is legitimate on condition that the loop slope at E_c does not essentially depend on E_m . This condition can be met. An example of the data on the thickness dependence of the loop tilt, which have been acquired while checking the validity of this condition, has been reported by Tagantsev *et al.* (Ref. 5).

⁵A. K. Tagantsev, M. Landivar, E. Colla, and N. Setter, in *Science and Technology of Electroceramic Thin Films*, NATO ASI, edited by O. Auciello and R. Waser (Kluwer Academic, Dordrecht, 1995), pp. 301–314.

⁶In several papers, it has been attempted to find the theoretical support for this spurious effect. However, this has been accomplished only at the

- expense of unjustified assumptions or outright mistakes. For example, in Ref. 7 it was implicitly assumed that at E_c an essential part of the polarization does not vanish (cf. Ref. 1 for a discussion). In Ref. 8, the depolarizing field is wrongly taken to be parallel—instead of antiparallel—to the direction of polarization.
- ⁷P. K. Larsen, G. J. M. Dormans, D. J. Taylor, and P. J. Vanvelthoven, *J. Appl. Phys.* **76**, 2405 (1994).
 - ⁸M. Dawber, P. Chandra, P. B. Littlewood, and J. F. Scott, *J. Phys.: Condens. Matter* **15**, L393 (2003).
 - ⁹J. F. M. Cillessen, M. W. J. Prins, and R. W. Wolf, *J. Appl. Phys.* **81**, 2777 (1997).
 - ¹⁰A. K. Tagantsev and I. A. Stolichnov, *Appl. Phys. Lett.* **74**, 1326 (1999).
 - ¹¹Note that, in this case, the total (measured) polarization of the system is not given by the charge on the electrode, which is equal to $P_f - \sigma$, since the variation of the latter is not fully controlled by the current in the external circuit.
 - ¹²J. Zhu, X. Zhang, Y. Zhu, and S. B. Desu, *J. Appl. Phys.* **83**, 1610 (1998).
 - ¹³S. P. Alpay, I. B. Misirlioglu, V. Nagarajan, and R. Ramesh, *Appl. Phys. Lett.* **85**, 2044 (2004).
 - ¹⁴M. W. Chu, I. Szafraniak, R. Scholz, C. Harnagea, D. Hesse, M. Alexe, and U. Gösele, *Nat. Mater.* **3**, 87 (2004).
 - ¹⁵I. P. Batra and B. D. Silverman, *Solid State Commun.* **11**, 291 (1972).
 - ¹⁶R. D. Tilley and B. Zeks, *Ferroelectrics* **134**, 313 (1992).
 - ¹⁷J. M. Ziman, *Principles of the Theory of Solids*, 2nd ed. (Cambridge University Press, Cambridge, 1972).
 - ¹⁸R. Kretschmer and K. Binder, *Phys. Rev. B* **20**, 1065 (1979).
 - ¹⁹Making allowance for the background permittivity becomes important when the depolarizing effect is involved, cf. Ref. 20.
 - ²⁰A. K. Tagantsev, *Ferroelectrics* **69**, 321 (1986).
 - ²¹A. K. Tagantsev, E. Courtens, and L. Arzel, *Phys. Rev. B* **64**, 224107 (2001).
 - ²²Y. Yamada, G. Shirane, and A. Linz, *Phys. Rev.* **177**, 848 (1969).
 - ²³Actually, the correlation length is anisotropic, i.e., the parameter δ —cf. Eq. (2.19)—is different for different orientations of the polarization and of its gradient. Since we are now interested in an estimate, we neglect this anisotropy in our consideration.
 - ²⁴O. G. Vendik and S. P. Zubko, *J. Appl. Phys.* **88**, 5343 (2000).
 - ²⁵S. K. Streiffer, C. Basceri, C. B. Parker, S. E. Lash, and A. I. Kingon, *J. Appl. Phys.* **86**, 4565 (1999).
 - ²⁶C. Basceri, S. K. Streiffer, A. I. Kingon, and R. Waser, *J. Appl. Phys.* **82**, 2497 (1997).
 - ²⁷O. G. Vendik and S. P. Zubko, *J. Appl. Phys.* **82**, 4475 (1997).
 - ²⁸J. Junquera and P. Ghosez, *Nature (London)* **422**, 506 (2003).
 - ²⁹N. A. Pertsev, A. G. Zembilgotov, and A. K. Tagantsev, *Phys. Rev. Lett.* **80**, 1988 (1998).
 - ³⁰A. Kopal, P. Mokry, J. Fousek, and T. Bahnik, *Ferroelectrics* **223**, 127 (1999).
 - ³¹A. M. Bratkovsky and A. P. Levanyuk, *Phys. Rev. Lett.* **80**, 3177 (2000).
 - ³²A. M. Bratkovsky and A. P. Levanyuk, *Phys. Rev. B* **63**, 132103 (2001).
 - ³³P. Mokry, A. K. Tagantsev, and N. Setter, *Phys. Rev. B* **70**, 172107 (2004).
 - ³⁴P. Mokry and A. K. Tagantsev (unpublished).
 - ³⁵A. K. Tagantsev, I. Stolichnov, N. Setter, and J. S. Cross, *J. Appl. Phys.* **96**, 6616 (2004).
 - ³⁶M. Grossmann, O. Lohse, D. Bolten, U. Boettger, T. Schneller, and R. Waser, *J. Appl. Phys.* **92**, 2680 (2002).
 - ³⁷M. Grossmann, O. Lohse, D. Bolten, U. Boettger, and R. Waser, *J. Appl. Phys.* **92**, 2688 (2002).
 - ³⁸J. J. O'Dwyer, *The Theory of Electrical Conduction and Breakdown in Solid Dielectrics* (Clarendon, Oxford, 1973).
 - ³⁹This analysis is related to the case of positive E_d ; in the general case, Eq. (2.58) should be taken with $|E_d|$ instead of E_d . This obviously does not affect the results of our analysis.
 - ⁴⁰I. L. Baginskii and E. G. Kostov, *Phys. Status Solidi A* **91**, 705 (1985).
 - ⁴¹We neglect the sign in the expression for V_{off} since, in practice, the sign of the voltage applied to a capacitor is fixed by convention. For a given convention, the sign of V_{off} can be determined from simple electrostatic arguments.
 - ⁴²C. J. Brennan, *Integr. Ferroelectr.* **7**, 93 (1995).
 - ⁴³J. G. Simmons, *J. Phys. Chem. Solids* **32**, 2581 (1971).
 - ⁴⁴Note that while κ_f , the dielectric constant of the ferroelectric, is a function of temperature, κ_i is the value of $\kappa_f(T)$ at the electrochemical equilibrium temperature.
 - ⁴⁵A. K. Tagantsev, C. Pawlaczyk, K. Brooks, and N. Setter, *Integr. Ferroelectr.* **4**, 1 (1994).
 - ⁴⁶The model discussed here is oversimplified—e.g., the electrodes and nearby-electrode regions of the ferroelectric are considered as electrochemically identical, and electrochemical equilibrium may not be reached at the deposition or top-electrode annealing temperature. However, these factors should not influence the validity of the qualitative picture of the phenomenon described by the model.
 - ⁴⁷J. F. Scott, C. A. P. de Araujo, B. M. Melnick, L. D. McMillan, and R. Zuleeg, *J. Appl. Phys.* **70**, 382 (1991).
 - ⁴⁸R. Waser and M. Klee, *Integr. Ferroelectr.* **2**, 23 (1992).
 - ⁴⁹C. J. Brennan, *Integr. Ferroelectr.* **2**, 73 (1992).
 - ⁵⁰A. M. Bratkovsky and A. P. Levanyuk, *Phys. Rev. B* **61**, 15042 (2000).
 - ⁵¹A. K. Tagantsev, V. O. Sherman, K. F. Astafiev, J. Venkatesh, and N. Setter, *J. Electroceram.* **11**, 5 (2003).
 - ⁵²The dislocation population can be controlled during processing—cf., e.g., T. Yamada, K. F. Astafiev, V. O. Sherman, A. K. Tagantsev, P. Murali, and N. Setter, *Appl. Phys. Lett.* **86**, 142904 (2005).
 - ⁵³A. K. Tagantsev, *Phys. Rev. B* **34**, 5883 (1986).
 - ⁵⁴A. K. Tagantsev, *Phase Transitions* **35**, 119 (1991).
 - ⁵⁵S. M. Kogan, *Sov. Phys. Solid State* **5**, 2069 (1964).
 - ⁵⁶W. Ma and L. E. Cross, *Appl. Phys. Lett.* **79**, 4420 (2001).
 - ⁵⁷For the sake of clarity, we will henceforward make the approximation $\epsilon_M^*/a_s \approx \epsilon_M^*/a$, which does not affect the essential features of the argument.
 - ⁵⁸K. Abe, S. Komatsu, N. Yanase, K. Sano, and T. Kawakubo, *Jpn. J. Appl. Phys., Part 1* **36**, 5846 (1997).
 - ⁵⁹K. Abe, N. Yanase, T. Yasumoto, and T. Kawakubo, *J. Appl. Phys.* **91**, 323 (2002).
 - ⁶⁰K. Abe, N. Yanase, T. Yasumoto, and T. Kawakubo, *Jpn. J. Appl. Phys., Part 1* **41**, 6065 (2002).
 - ⁶¹W. J. Merz, *Phys. Rev.* **95**, 690 (1956).
 - ⁶²R. Landauer, *J. Appl. Phys.* **28**, 227 (1957).
 - ⁶³A. K. Tagantsev, *Ferroelectrics* **184**, 79 (1996).
 - ⁶⁴M. Molotskii, R. Kris, and G. Rosenman, *J. Appl. Phys.* **88**, 5318 (2000).
 - ⁶⁵G. Gerra, A. K. Tagantsev, and N. Setter, *Phys. Rev. Lett.* **94**, 107602 (2005).
 - ⁶⁶The following expression for c is valid when the argument of the logarithmic function is much greater than unity, which is typically the case for ferroelectrics.
 - ⁶⁷A. P. Levanyuk and A. S. Sigov, *Defects and Structural Phase Transitions* (Gordon and Breach, New York, 1988).
 - ⁶⁸The thermodynamic coercive field introduced in this way is the field at which the antiparallel orientation of polarization relative to the applied field becomes absolutely unstable with respect to an infinitesimal increment of the polarization in the longitudinal direction. One should note that such quantity may not be the real thermodynamic coercive field of the system if more than two antiparallel domain states are involved in the switching—cf. Ref. 69.
 - ⁶⁹M. Iwata and Y. Ishibashi, *Jpn. J. Appl. Phys., Part 1* **38**, 5670 (1999).
 - ⁷⁰T. Yamamoto, *Jpn. J. Appl. Phys., Part 1* **35**, 5104 (1996).
 - ⁷¹A. K. Tagantsev, I. Stolichnov, N. Setter, J. S. Cross, and M. Tsukada, *Phys. Rev. B* **66**, 214109 (2002).
 - ⁷²Y. Imry and S. Ma, *Phys. Rev. Lett.* **35**, 1399 (1975).
 - ⁷³A. M. Bratkovsky and A. P. Levanyuk, *Phys. Rev. Lett.* **94**, 107601 (2005).
 - ⁷⁴A similar result was previously found by Glinchuk and Morozovska (Ref. 75), who considered the poling effect of the lattice mismatch between ferroelectric and substrate. In this case, the smearing of the phase transition is less pronounced, as the effect is proportional to the square of the misfit strain (typically less than 1%). Moreover, the relation between misfit strain and surface polarization in Eqs. (5) and (7) of Ref. 75 is incorrect: it is the latter quantity that is induced by the former via the piezoelectric effect, and not the other way around, so that strain should be multiplied—and not divided—by the piezoelectric coefficient to get the induced polarization!
 - ⁷⁵M. D. Glinchuk and A. N. Morozovska, *J. Phys.: Condens. Matter* **16**, 3517 (2004).
 - ⁷⁶R. Takayama and Y. Tomita, *J. Appl. Phys.* **65**, 1666 (1989).
 - ⁷⁷D. Dimos, W. L. Warren, M. B. Sinclair, B. A. Tuttle, and R. W. Schwartz, *J. Appl. Phys.* **76**, 4305 (1994).
 - ⁷⁸A. L. Kholkin, K. G. Brooks, D. V. Taylor, S. Hiboux, and N. Setter, *Integr. Ferroelectr.* **22**, 1045 (1998).
 - ⁷⁹M. Alexe, C. Harnagea, D. Hesse, and U. Gösele, *Appl. Phys. Lett.* **79**, 242 (2001).

- ⁸⁰S. Traynor, T. Hadnagy, and L. Kammerdiner, *Integr. Ferroelectr.* **16**, 63 (1997).
- ⁸¹K. Abe, N. Yanase, and T. Kawakubo, *Jpn. J. Appl. Phys., Part 1* **39**, 4059 (2000).
- ⁸²In the original paper, Ref. 77, a relation was used in the discussion which predicts a linear thickness dependence of V_{off} . This relation, Eq. (1), is valid only in the absence of charges on the electrodes. The formula taking into account these charges, Eq. (2.54) in the present paper, does not predict such dependence.
- ⁸³K. Carl and K. H. Hardtl, *Ferroelectrics* **17**, 473 (1978).
- ⁸⁴E. G. Lee, D. J. Wouters, G. Willems, and H. E. Maes, *Appl. Phys. Lett.* **70**, 2404 (1997).
- ⁸⁵S. Hiboux and P. Muralt, *Integr. Ferroelectr.* **36**, 83 (2001).
- ⁸⁶S. Hiboux, Ph. D. thesis, Swiss Federal Institute of Technology (EPFL), 2001.
- ⁸⁷J. Lee, R. Ramesh, V. G. Keramidas, W. L. Warren, G. E. Pike, and J. T. Evans, *Appl. Phys. Lett.* **66**, 1337 (1995).
- ⁸⁸G. E. Pike, W. L. Warren, D. Dimos, B. A. Tuttle, R. Ramesh, J. Lee, V. G. Keramidas, and J. T. Evans, *Appl. Phys. Lett.* **66**, 484 (1995).
- ⁸⁹W. L. Warren, D. Dimos, G. E. Pike, B. A. Tuttle, M. V. Raymond, R. Ramesh, and J. T. Evans, *Appl. Phys. Lett.* **67**, 866 (1995).
- ⁹⁰P. Schorn, U. Ellerkmann, D. Bolten, U. Boettger, and R. Waser, *Integr. Ferroelectr.* **53**, 361 (2003).